DESIGN OF CONTROLLER FOR GRID CONNECTED PHOTOVOLTAIC SYSTEM

A PROJECT REPORT

SUBMITTED PARTIAL FULFILLMENT OF THR REQUIREMENTS FOR THE AWARD OF THE DEGREE

OF

MASTER OF TECHNOLOGY

IN

POWER SYSTEM

Submitted by

MUSTAFA ELTIGANI IBRAHIM MOHAMMED

2K20/PSY/22

Under the supervision of

PROF. UMA NANGIA

DEPARTMENT OF ELECTRICAL ENGINEERING

DELHI TECHNOLOGICAL UNIVERSITY

NEW DELHI, 110042, DELHI (INDIA)

May. 2022

DELHI TECHNOLOGICAL UNIVERSITY

(Formerly Delhi College of Engineering)

Bawana Road, Delhi-110042

CANDIDATE'S DECLARATION

I, Mustafa Eltigani Ibrahim Mohammed, Roll No. 2K20/PSY/22 of Master of Technology (M.Tech) Power System, hereby declare that the project dissertation titled "Design of Controller for Grid Connected Photovoltaic System" which is submitted by me to the Department of Electrical Engineering, Delhi Technological University, Delhi in partial fulfillment of the requirement for the award of the degree of Master of Technology is original and copied from any source without proper citation. This work has not previously formed the basis for the award of any Degree, Diploma Associateship, Fellowship, or other similar title or recognition

Place: Delhi, India

Date: 20 . May .2022

Mustafa Eltigani Ibrahim Mohammed

Roll No. 2K20/PSY/22

M.Tech Power System Engineering

Dept. Electrical Engineering

Delhi Technological University

New Delhi – 110042, India

DELHI TECHNOLOGICAL UNIVERSITY

(Formerly Delhi College of Engineering)

Bawana Road, Delhi-110042

CERTIFICATE

I hereby certify that the Project Dissertation titled “Design of Controller for Grid Connected Photovoltaic System “which is submitted by Mustafa Eltigani Ibrahim Mohammed, Roll No. 2K20/PSY/22, Department of Electrical Engineering, Delhi Technological University, Delhi in partial fulfillment of the requirement for the award of the degree of Master of Technology, is a record of the project work carried out by the student under my supervision. To the best of my knowledge this work has not been submitted in part or full for any Degree or Diploma to this University or elsewhere.

Place: Delhi, India PROF. UMA NANGIA

Date: 20 . May.2022 SUPERVISOR

ACKNOWLEGEMENT

I would like to thank my Supervisor PROF. UMA NANGIA who guided us in doing these projects. He provided us with invaluable advice and helped us in difficult periods. His motivation and help contributed tremendously to the successful completion of the project. Special thanks to The Indian Council for Cultural Relations (ICCR) to offer my scholarship scheme.

Also, I would like to thank my family and friends for their support. Without that support, we couldn't have succeeded in completing this project.

Mustafa Eltigani Ibrahim Mohammed

Roll No. 2K20/PSY/22

M.Tech Power System Engineering

Dept. Electrical Engineering

Delhi Technological University

New Delhi – 110042, India

ABSTRACT

Growing environmental concerns and the depletion of conventional energy supplies reserves such as fossil fuel, photovoltaic energy sources have greatly increased in recent decades. Furthermore, this sort of power source offers other benefits such as low pollution, dependability, availability, no mechanical moving parts, less maintenance, a long-life span, and silence. More solar energy sources are expected to collaborate with a grid in the future. Aside from the low performance of a photovoltaic source of energy, the fundamental problem of a grid interfaced-based photovoltaic system is its controllability. As the result, power energy produced from photovoltaic energy sources can be untracked at the maximum power point, if the system is not appropriately adjusted. Therefore, the optimization tracking techniques applied to the photovoltaic energy source become of high interest and always important for the sake of accomplishing excellent power quality and highest reliability.

This dissertation presents the management active and reactive power of a single-phase PV system grid connected designed by an intelligent PSO-PID controller and hybrid fuzzy logic fraction order proportional-integral controller (FLCFOPI Controller). Intelligent PSO-PID Controller employed to MPPT to control PV voltage and optimize the performance of tracking power produced by PV panel, a hyperbolic cosine non-linear gain adds to the integral gain of PID controller to reduce large error in I-V characteristic curve of PV. The hybrid fuzzy logic fraction order proportional-integral controller (FLCFOPI Controller) is employed to single-phase full-wave H-bridge voltage source inverter (VSI) with SPWM which aims to maintain dc-link voltage, unity power factor, and reduce voltage ripple. Single-phase lock loop (PLL) based 1/4 transport delay method is used to synchronize the phase of the PV- VSI with the grid-connected system. The proposed controller provides maximum active power into the grid while maintaining a power factor of unity, and it also allows for the modification of reactive power pumped into the system. The simulation result findings the proposed controller has a fast-settling time, robustness, and ability to tack grid power. For the validation of the effectiveness, efficiency, and validity of the proposed model the simulation results have been accomplished through MATLAB/ Simulink simscope power system.

TABLE OF CONTENTS

LIST OF TABLES

LIST OF FIGURES

CHAPTER 1 INTRODUCTION

1.1 Overview

The main goal of this chapter is to present the motivation and background of this dissertation. It also introduces photovoltaic cells, the Maximum Power Point Tracking (MPPT) method, a DC-DC Boost Converter for a photovoltaic system, and a Single Phase Voltage Source Inverter (VSI) with two legs, and a Single-Phase Grid-Connected PV System. Figure 1. A grid-connected photovoltaic renewable resource is made up of energy transducers such as a solar panel, dc-dc boost converter to raise photovoltaic voltage, and dc-ac Inverter to link the photovoltaic (PV) source of power to the utility grid. Furthermore, the structure of this dissertation allows for a more in-depth comprehension of the topic matter. At the end of this dissertation, there is a list of publications pertinent to this issue.

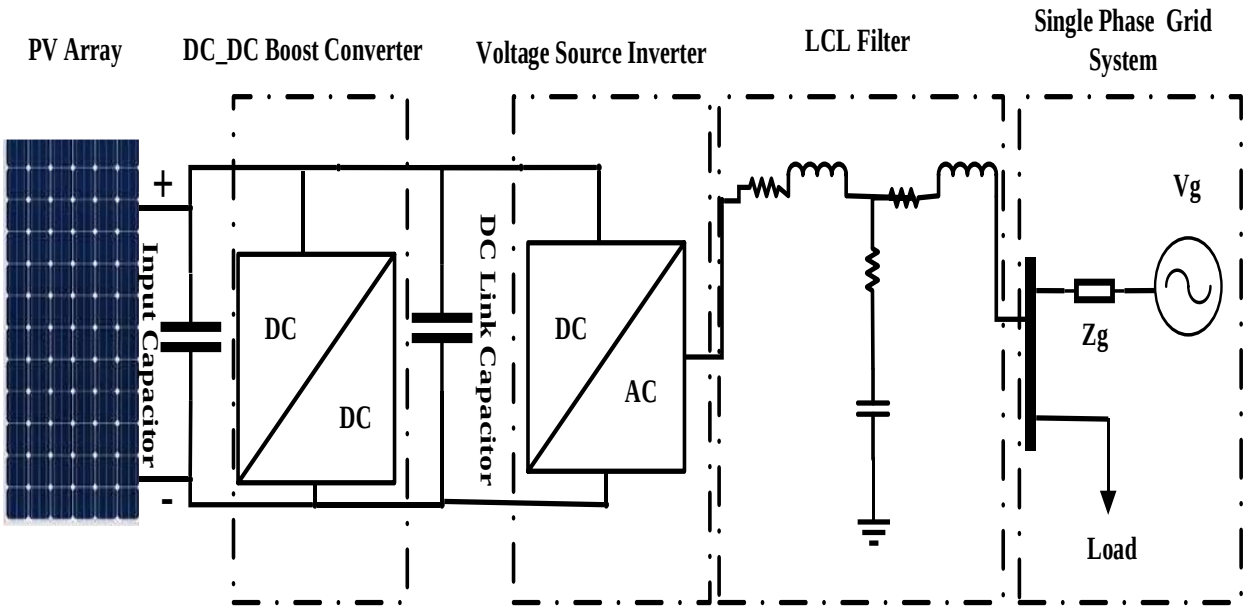

Fig 1.1 Scheme of Photovoltaic System with grid Connected

1.2 BACKGROUND AND LITERATURE REVIEW

Electric power demand is expanding globally in tandem with population growth, posing a challenge for governments to meet the increase in load consumption using existing power generating and distribution systems. The planning process and the economy are the two most significant problems. Large power plants need extensive planning and are time-consuming to

construct. Furthermore, because such planning is resource-demanding, it may not be profitable to provide the dispersion load or remote load. New techniques of electricity distribution are in high demand, and if well planned, they can solve the aforementioned obstacles [1]. Because of the high request for energy and lacking resource capacity of fuel, the researchers go to green energy sources such as renewable energy, fossil fuel, wind turbine, and ocean thermal energy to cover the limitation of resources. Nowadays green energy is an important resource of generation energy that has less maintenance [2]. Solar energy is the perfect source of generating energy from green energy which use photovoltaic cell to generate electrical energy. The energy produced from the PV system is considered a long-term resource in grid connection system which doesn't require fuel cost, the main principle of a Photovoltaic System (PV) is to adapt the sunlight to electrical power energy by the photovoltaic effect, however, it has non-linear behavior depend on the appearances of power - voltage (P-V) and current-voltage (I-V) this behavior effect by irradiation and temperature [2,3].

1.3 PHOTOVOLTAIC CELL MODELING

A photovoltaic is a p-n junction made from semi-conductor diode materials that work by the photovoltaic effect, there are different types of semiconductors used depending on the manufacturing, polycrystalline and monocrystalline commonly used to build PV cells. A single photovoltaic panel approximately produces 5W at 0.5V DC. Which need to be linked in parallel or series or series-parallel to increase power generation from the cell. The characteristics of PV depend on the irradiation and temperature respective to the load condition; which operation on maximum power point (MPP). They are different models of PV cells introduced in literature [4,5]. A single diode PV cell type is widely used to build PV solar systems. PV cells must be coupled in series-parallel arrangements to increase the output. In general, PV cells are linked in series to provide a voltage level that fits the power processing system's requirement specification. The required power level of the Photovoltaic system is achieved by joining several strings in parallel, resulting in a rise in the PV field's current rate [6]. Figure 1.2 shows the structure model PV cell.

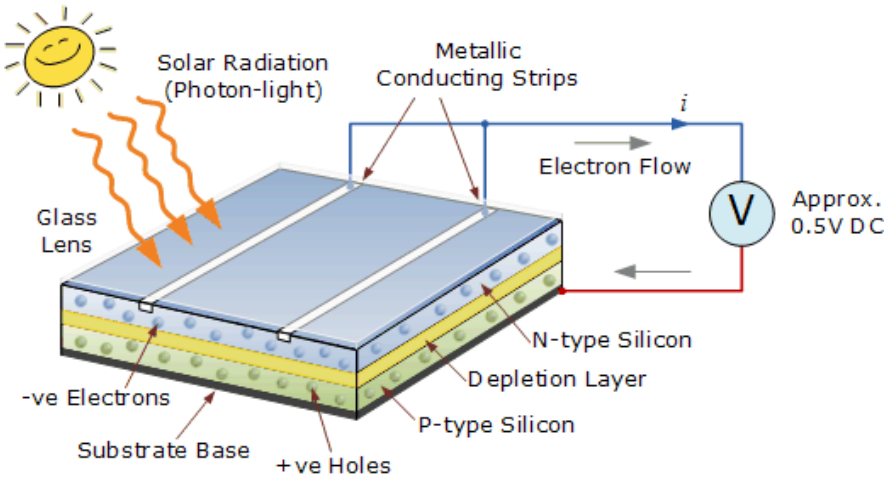

Fig 1.2 Structure of Photovoltaic Cell

1.4 MAXIMUM POWER POINT TRACKING MOTHED

It is difficult to maintain generated PV energy power at the optimal operation point due to variations in environmental conditions; in reality, that maximum power point (MPP) gradually fluctuates with solar insolation. As a result, the PV system requires a controller device to optimize the operational parameters of the MPP through the use of an MPPT system. The photovoltaic module has non-linear dynamic characteristics of voltage, current, and changes in weather condition which means temperature and irradiation, therefore the MPPT has been implemented to ensure the power energy generation for the photovoltaic cell is working on (MPP) with considering changes in temperature and irradiation, without MPPT the voltage load delivered by photovoltaic zero which can be understood from characteristic curve of solar panel. MPPT is a final control mechanism used in an energy conversion system between solar panels and a solar transformer to improve the powerful energy of the photovoltaic module. In recent decades, several MPPTs algorithm solutions have been explored and developed to increase the power efficiency of photovoltaic panels operation under diverse atmospheric conditions. [7]. Intelligent PSO-PID controller-based MPPT algorithms are connected to the PV system in this work to maintain solar modules operating at MPP regardless of environmental circumstances. The benefits of this method include quick dynamic reaction, imprecise system control, resilience, and the absence of the necessity for correct mathematical formulation. Furthermore, in comparison to Particle Swarm Optimization Algorithm (PSO) and the Perturbation and Observation Algorithm (P&O) (P and O).

Under rapidly changing air circumstances, this method can properly monitor the MPP with low oscillation.

1.5 GRID CONNECTED PHOTOVOLTAIC SYSTEM

Because of advancements in power electronics equipment, the demand for PV systems connected to utilities is rapidly expanding. Nonetheless, the PV system has low efficiency as a result of linking a solar energy source to a power grid, which may affect performance if the infrastructure is not correctly designed [8]. To ensure the reliability and stability of the electricity sent to the grid, the adaptive control architecture for the Photovoltaic system's inverter linked to the power network must perform the following functions:

- Optimize the power efficiency generated by a photovoltaic system by tacking the MPP, which may be achieved by employing the MPPTs algorithm.
- A photovoltaic inverter output current injected into the utility grid should be in phase with utility grid voltage and exhibits lower switching frequency ripples and lower harmonic distortion, therefore the unity power factor operation can be maintained.

The suggested technique for a one-phase full-wave rectifier inverter with unipolar Sinusoidal Pulse Width Modulation (SPWM) contains two controllers: a voltage-controlled feedback control that can provide voltage stability at the dc link and a current control loop that is being used to create sinusoidal as well as keep the control performance at unity power factor. The LCL filter was employed to reduce the switching frequency ripples injected into the utility as a consequence of the solar inverter output current.

1.6 Objectives and Major Contributions of this Dissertation

The purpose of this dissertation is to design a controller technique for the single-phase double-stage grid-connected photovoltaic energy source to improve efficiency and reduce cost. The major contribution of this research can be briefed as in the following point:

1. Design of PID Controller using PSO for MPPT application, to enhance the dynamic performance and ensure maximum power following regardless of changing of the atmospheric condition.
2. Comparison of proposed MPPT controller with other optimization techniques.

3. Design control for the Voltage Source Inverter (VSI-SPWM) with grid stability.
4. Design Phase Lock Loop (PLL) grid Synchronization algorithm.
5. Design Techniques of an LCL filter, which is connected between the output of VSI and the grid system to reduce ripples along with the inverter output current.
6. Design DC-link Capacitor with voltage ripple Controller.

1.7 Dissertation Outline

The dissertation chapters are arranged as follows to achieve the aforementioned goal and make this research's main contribution:

Chapter 1. Introduction. This chapter describes introduces the background and motivation of photovoltaic technology and its applications and objective of this dissertation and the contents of its chapter.

Chapter 2. Photovoltaic Cell Modeling and Characteristic, this chapter describes the equivalent electrical circuit illustration of a photovoltaic cell and mathematical models based on a single diode type model. MATLAB software is utilized to simulate the dynamic behaviors of a photovoltaic module under changing atmospheric conditions. Simulation results indicate better engagement concerning the datasheet provided by manufacturers and other related works.

Chapter 3. Maximum Power Point Tracking (MPPT) Techniques, this chapter presents the design of the dc-dc boost converter and the design of the proposed Maximum Power Point Algorithm based on an intelligent PSO-PID controller for optimizing power efficiency and comparing with Particle Swarm Optimization Techniques (PSO).

Chapter 4. Design Controller for Single Phase Grid Connected PV System, this chapter presents a design strategy for a single-phase voltage source inverter 2 legs based on SPWM controller, size of DC link capacitor, voltage and current regulator, Phase Lock Loop (PLL) grid Synchronization algorithm**,** and LCL filter.

Chapter 5. The Result, Discussion, and Conclusion, this chapter present the output result of the proposed controller and system under testing conditions then discuss the result, and finally ill summarizes all the contribution work in the conclusion section.

CHAPTER 2 PHOTOVOLTAIC CELL MODELING AND CHARACTERISTIC

2.1 Overview

A photovoltaic cell can use a solar panel to generate electricity from sunlight. Using the electronic characteristics of semiconductor materials, convert sunlight into P-V transition. The item is simple to install as consumer life lights. In certain industrialized nations, it may also be utilized in combination with the global electricity network to establish redundancy. A solar cell is simply a P-N junction made up of two independent layers of silicon loaded with a minuscule number of atoms: atoms with one more valence electron, known as donors, and atoms with one less valence electron, known as acceptors, in the case of the n-layer. When the thin sheets are joined, the N-free layer's electrons seep into the P-side at the junction, leaving a positively charged area behind. Similarly, the open pores in the P-layer scatter on the N-side, producing a negative charges patch behind the acceptors. This generates an electrical charge between both sides, which may act as a barrier against further transit [9].

2.2 Modeling of Photovoltaic Cell

A photovoltaic cell is essentially a p-n connection diode that generates an electric charge when an incoming photon has greater energy than the electronic component element's energy bandgap. Because a single solar cell has a limited output power, a photovoltaic module is coupled in shunt and series mode to form a PV cell. Cell circuit layouts are divided into three varieties based on the number of diodes used: one diode, two diodes, and three diodes. The double and three diode forms are quite tough, while the single-mode form is simple and uncomplicated. Figure 2.1 displays the equivalent circuit of a single diode-type photovoltaic cell.

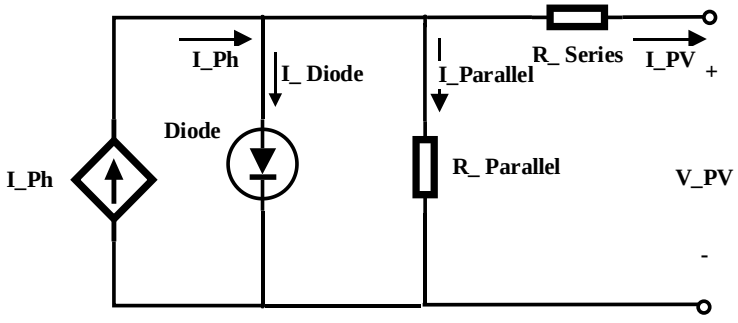

Fig. 2.1 Equivalent Circuit of Single Photovoltaic cell

The output current produced from the PV array is given by equation (2.1)

$$I_{pv} = I_{ph}N_p - I_{diode}N_p\left[\exp\left(\frac{q\left(\frac{V_{pv}}{N_s} - \frac{I_{pv}R_{series}}{N_p}\right)}{AKT}\right) - 1\right] - \left(\frac{\frac{V_{pv}N_p}{N_s} + I_{rs}}{R_{parallel}}\right) \quad (2.1)$$

Where is:

I_{pv} = output photovoltaic current

I_{ph} = photocurrent produced from the solar array

I_{diode} = diode current

I_{rs} = reverse saturation current of the diode

N_p = number of PV cells connected in parallel to the PV cell

N_s = number of PV cells connected in series of the PV cell

R_{series} , $R_{parallel}$ = series and parallel resistance respectively

V_{pv} = output photovoltaic voltage

K = Boltzmann constant ($1.38\times10^{-23}\ J/K$)

q= electron charge ($1.6\times10^{-19}\ C$)

T= Temperature in Kelvin

The photovoltaic device manufacturer generally does not provide the all data of the one-diode model. Manufacturers generally provide datasheets including the following data of the photovoltaic panels STC; temperature coefficient (K_v) of an open circuit voltage (V_{oc}) , short circuit current (I_{sc}),

MPP voltage and MPP current (V_{mmp}, I_{mmp}), temperature factor of short circuit current (K_i), MPP power (P_{mmp}), and open-circuit voltage (V_{oc}). Therefore, most manufacturers provide a set of voltage-current curves (I-V) and voltage power curves (P-V) for irregular atmospheric conditions, based on the investigation of the photovoltaic model in the operation point of the I-V dynamic curve, (V_{oc}), MPP power (P_{mmp}) and short circuit current (I_{sc}). Allows relating the information provided by the datasheet to unknown parameters of an electrical model. At the short circuit condition, the photovoltaic module an open circuit voltage (output voltage) is equal to zero, therefore, from equation (2.1) the short circuit current (I_{sc}) can be found by equivalence (2.2)

$$I_{sc} = I_{ph} - I_{rs}\left(\exp\left(\frac{IR_s}{N_s v_t}\right) - \frac{IR_{series}}{R_{parallel}}\right) \tag{2.2}$$

Since the value of (I_{ph}) is much greater than (I_{rs}) neglecting the leakage-ground current at a short circuit state, (I_{sc}) s almost similar to a photogenerated current (I_{ph}) thus can understand equation (2.2) be simplified $(I_{sc} = I_{pv})$, In contrast, the open-circuit voltage parameter can be attained by neglecting the output current (equal to nothing). an open circuit voltage at a short circuit condition correlated to the temperature of the photovoltaic module can be written as in equation (2.3).

$$V_{oc} = V_{oc,stc} + K_v(T - T_{ref}) \tag{2.3}$$

The diode reverse saturation current (I_o) is most often obtained by the use of equation (2.2) as follows.

$$I_{rs} = \frac{I_{ph} - V_{oc} / R_{parallel}}{\exp(V_{oc} / V_t) - 1} \tag{2.4}$$

There is another method usually used in parameter estimation techniques is based on equation (2.2) in the MPP.

$$I_{mpp} = I_{ph} - I_{rs}\left(\exp\left(\frac{V_{mpp} + I_{mpp}R_{series}}{N_s V_t}\right) - 1\right) - \frac{V_{mpp} + I_{mpp}R_{series}}{R_{parallel}} \tag{2.5}$$

2.3 Parameter Estimation Method of Solar Photovoltaic System

Because of its precision and flexibility, the single diode PV type has been used in the majority of investigations for estimating electrical values of the parameters [10,11]. Recently many researchers focusing on unknown paraments of the photovoltaic cell. in this section, we discuss two types of estimation techniques which are Xiao's Technique and Villalva's Technique.

2.3.1 Xiao's Method

This approach is driven by the fact that the output power of a photovoltaic module is equivalent to zero at an MPP, larger than zero on an MPP left side, and less than zero on an MPP right side when compared to the output voltage of a photovoltaic module [12]. Based on this approach we can rewrite equations (2.4) and (2.5) by equation (2.6) and (2.7) by negligible parallel resistance ($R_{parallel}$).

$$I_{rs} = \frac{I_{ph}}{\exp\left(V_{oc} / V_t\right) - 1} \tag{2.6}$$

$$I_{mpp} = I_{ph} - I_{rs}\left(\exp\left(\frac{V_{mpp} + I_{mpp}R_{series}}{N_s V_t}\right) - 1\right) \tag{2.7}$$

By subsisting equations (2.6) and (2.7) we can find the result in equation (2.8)

$$I_{mpp} = I_{ph} - \left(\frac{\exp\left(\frac{V_{mpp} + I_{mpp}R_{series}}{N_s V_t}\right) - 1}{\exp\left(\frac{V_{oc}}{V_t}\right) - 1}\right) I_{ph} \tag{2.8}$$

By rearranging equation (2.8) we can obtain the formula for R_{series}

$$R_{series} = \frac{V_t In\left(\left(1 - \frac{I_{mpp}}{I_{ph}}\right)e^{(V_{oc}/V_t)} + \frac{I_{mpp}}{I_{ph}}\right) - V_{mpp}}{I_{mpp}} \tag{2.9}$$

By considering the change in PV power respective to PV voltage equal to zero;

$$\frac{dP_{pv}}{dV_{pv}} = 0 = \frac{I_{mpp}}{V_{mpp}} - \left(\frac{\frac{I_{rs}}{V_t} e^{\left(\frac{V_{mpp}+I_{mpp}R_{series}}{Vt} \right)}}{1+\frac{I_{rs}R_{series}}{V_t} e^{\left(\frac{V_{mpp}+I_{mpp}R_{series}}{Vt} \right)}} \right) \tag{2.10}$$

Mathematical equations (2.10) determine the four variables in this approach. Therefore (I_{ph} , I_{rs} , and R_{series}) reduce the right side of equation (2.10) which represents the estimated parameters of the PV module.

2.3.2 Villalva's Method

When iteration begins, Villalva's approach allows just two factors R_{series} *and* $R_{parallel}$ to be retrieved concurrently while keeping the diode ideality factor unchanged. The retrieved parameter values are heavily influenced by the acceptability region and the R_{series} increase [12-13]. Assuming that the through certain may be chosen freely, they can be modified for an acceptable fit (I-V) curve beginning from a fixed value. The value of parallel resistance can determine as a function of series resistance, which shows in equation (2.11)

$$R_{parallel} = \frac{V_{mpp}\left(V_{mpp} + I_{mmp}R_{series}\right)}{V_{mpp}\left[I_{ph} - I_o\left(e^{\left(\frac{V_{mmp}+I_{mmp}R_{series}}{V_t} \right)} - 1 \right) \right] - P_{mpp}} \tag{2.11}$$

Considering equation (2.11), it is obvious that for each number of series resistant R_{series} , one value of shunt resistance $R_{Parallel}$ is produced, causing the electrical model to shift nearer to an operational point V_{mpp}*and* I_{mpp} specified in the datasheet. Moreover, the iterative response R_{series} *and* $R_{parallel}$ is used in this approach. Every iteration changes $R_{Parallel}$ in the direction of the best solution architecture [14].

$$I_{ph} = \left(\frac{R_{parallel} + R_{series}}{R_{Parallel}} \right) I_{sc} \tag{2.12}$$

The initial value of shunt resistance may be given by equation 2.13 and a starting value of series resistance equals zero. Since this is estimated by an author as

$$R_{sh,\min} = \frac{V_{mpp}}{I_{sc} - I_{mpp}} - \frac{V_{oc} - V_{mpp}}{I_{mpp}} \tag{2.13}$$

2.4 Characteristics of Photovoltaic Module

The cells are made in modules or multiple modules series and parallel connections these modules are used in a PV cell to achieve the required output energy of the modules; the dynamic behavior of a PV module can be described by the power-voltage (P-V) and current-voltage curves (I-V) [15-17]. The PV module must account for the influence of variation in the solar array (irradiance and temperature). The manufacturer provides all of the parameters for the solar module in the datasheet. The PV datasheet is presented in TABLE (2.1) in this thesis, and This data is used to compute the solar module characteristic curve during typical working circumstances.

TABLE 2.1: Manufactures datasheet of REC Solar REC325PE72 PV Panel

Photovoltaic Parameters	Rating Values
MPP Current (I_{mpp})	8.46 A
MPP Voltage (V_{mpp})	38.5 V
MPP Power (P_{mpp})	325.71 W
Short Circuit Current (I_{sc})	9.05 A
Open Circuit Current (V_{oc})	46.4 V
Temperature Coefficient of Voltage (K_v)	-0.32 V/C^o
Temperature Coefficient of Current (K_i)	0.06 A/C^o

2.4.1 Photovoltaic Cell Characteristic Under Changing in Solar Irradiation

The manufacturer provides (I-V) and (P-V) dynamic characteristic curves as a datasheet, these data show the dynamic behavior of change of cell insolation. To get the impacts of solar irradiance intensity on a photovoltaic module, the dynamic characteristics curve of a photovoltaic module ware measured in the different solar irradiance intensities ranging from 1000 W/m^2, 800 W/m^2, 600 W/m^2 through the measurement procedure, The surface temperature of the photovoltaic module was kept constant at 25^0 C. Figures 2.2 and 2.3 demonstrate this when the isolation drops, the short circuit current drops in direct proportion. This makes sense that the photovoltaic module-generated current is related to a photons flux directly. When the solar irradiance is low down, the photon flux is decreasing with the increasing solar irradiance leading to an increase in an open circuit voltage as well as short current increasing, hence an MPP varies [18]. Three PV cells are linked in parallel to create high power, and four PV panels are connected in series to generate low power.

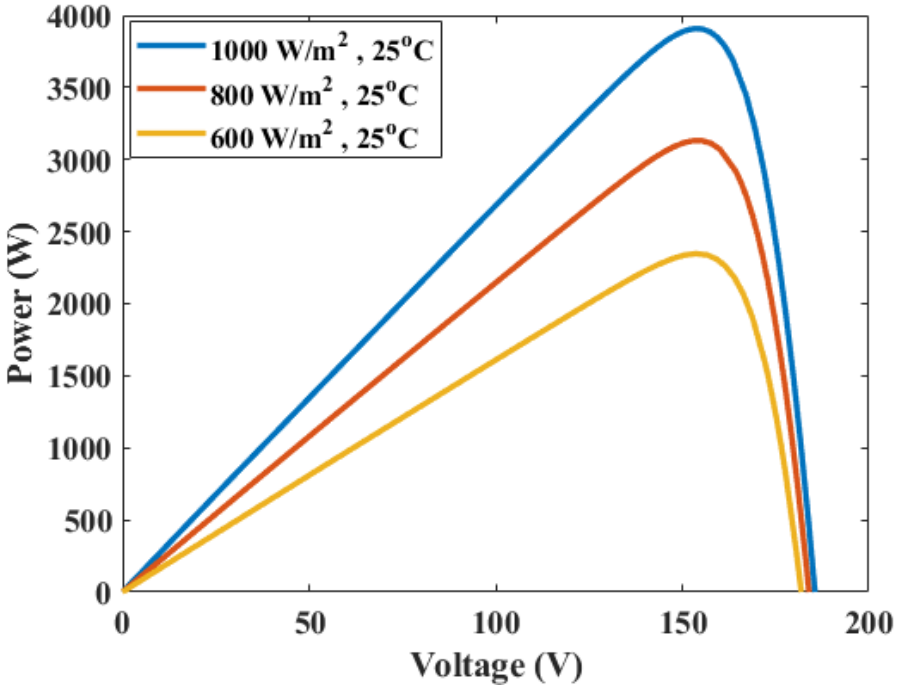

Fig 2.2 P-V Curve for PV System

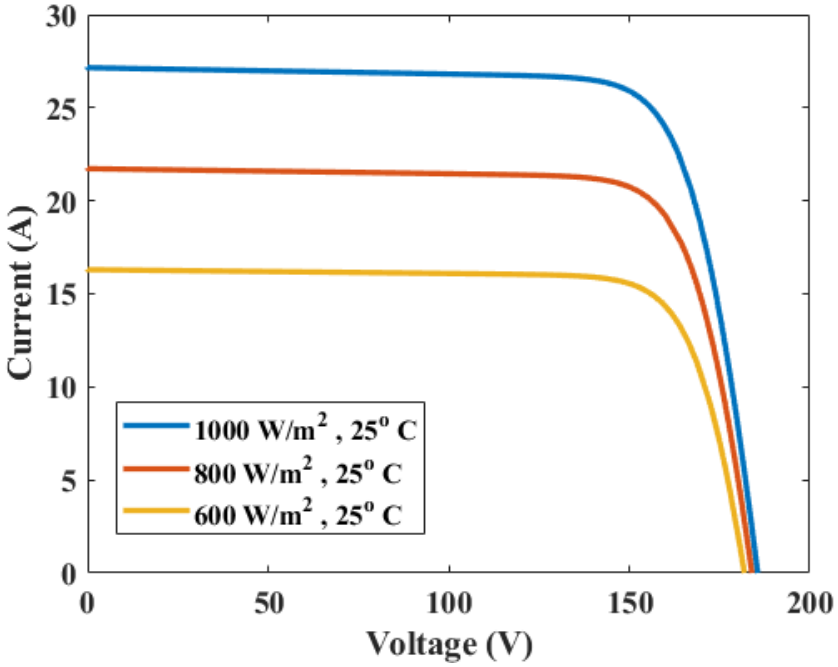

Fig 2.3 I-V Curve for PV System

2.4.2 Photovoltaic Cell Characteristic Under Changing in Temperature

The power energy efficiency of solar modules is influenced by temperature, The functionality of PV is impacted by temperature rises, which is dependent on temperature's linear operation. Therefore, A photovoltaic module's temperature has a huge impact on its performance [19]. As shown in Fig. 2.4 and Fig 2.5, the output current of a solar module in a short circuit situation is proportional to the temperature of the module; as the temperature rises, the short circuit current rises somewhat, but the open-circuit voltage decreases significantly. Nevertheless, one of the reasons the photovoltaic array operates efficiently at low temperatures is because semiconductor materials' energy gap varies with temperature.

Short circuit conditions, a reduction in the band of the energy gap, and an increase in the number of photons in the valence and conduction bands result in a modest rise in the output current, but large drops in the open-circuit voltage increase the leakage current. The gap energy of semiconductor materials increases as the temperature rises. Because charge carriers are discharged at a lower potential, photons in a conductive band will take more energy to migrate to the conduction band, resulting in a loss in photovoltaic output power given the same photogenerated current.

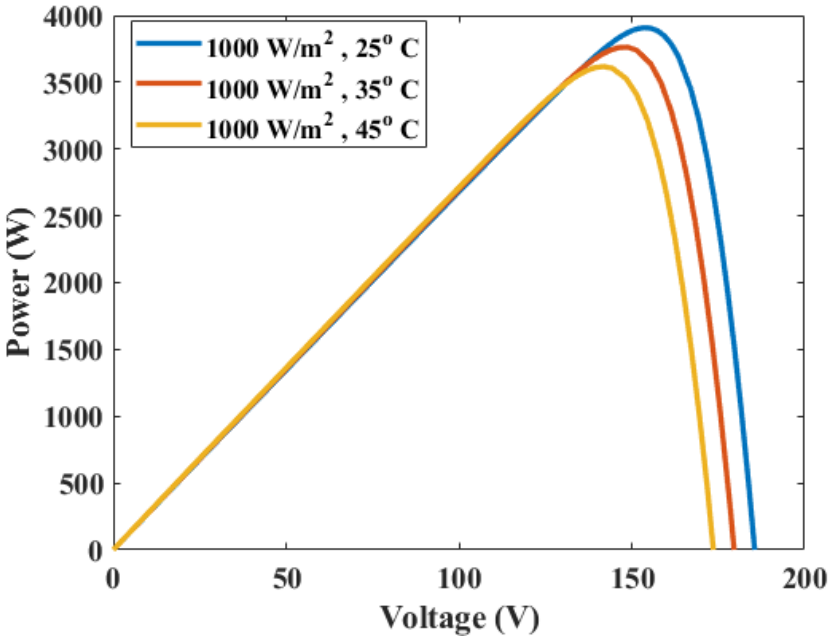

Fig 2.4 P-V Curve for PV System

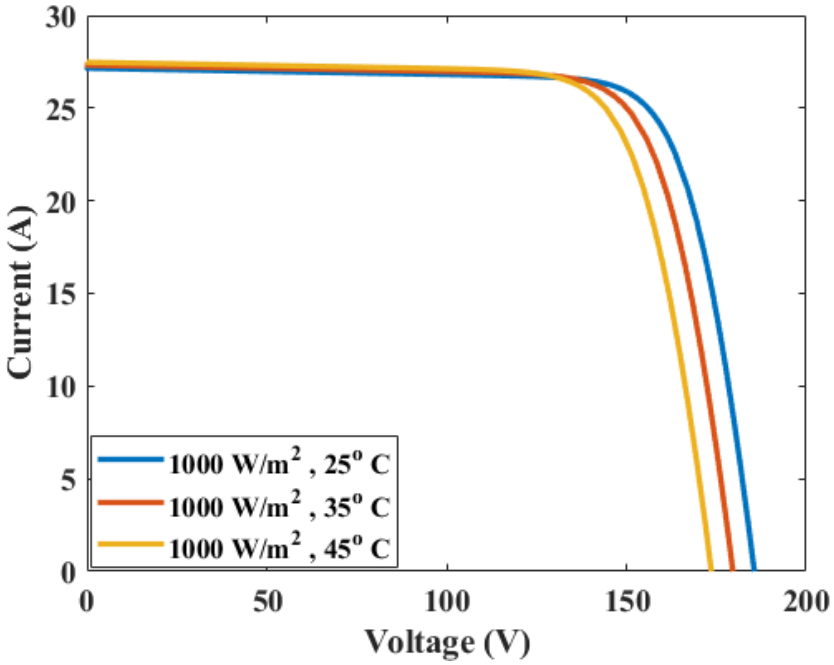

Fig 2.5 I-V Curve for PV System

CHAPTER 3 MAXIMUM POWER POINT TRACKING TECHNIQUES

3.1 Overview

Solar cells are designed to transfer solar radiation into electricity through the use of a power electronics device with nonlinear behavior that reduces efficiency. Because these characteristics are affected by climate change, It is critical to maximizing power production. [20]. The efficiency of the output power of the photovoltaic energy is ineffective if MPPT algorithm techniques were not sure the PV module operating at MPP, therefore during changing atmospheric conditions and steady-state conditions the total effectiveness of the output power produced by the photovoltaic energy source is depending on the output of the conversion efficiencies which should be implied by considering an MPPT algorithm efficiency and extremely variable operating condition during the day, basically the maximum power point tracking algorithm operation contingent on the solar irradiance [21-22].

3.2 Design of DC-DC Boost Converter

The dc-dc boost converter works with dc sources, such as dc generators, batteries, and photovoltaic arrays. DC to DC converter refers to the process of converting one DC voltage to another. A boost converter, in general, is a DC-to-DC converter having an output voltage larger than the input signal. In this project, the dc-dc converter regulates the voltage produced by PV cells and increases PV module voltage. This output voltage is subject to the duty cycle controlled by varying switching ON time on the switching device.

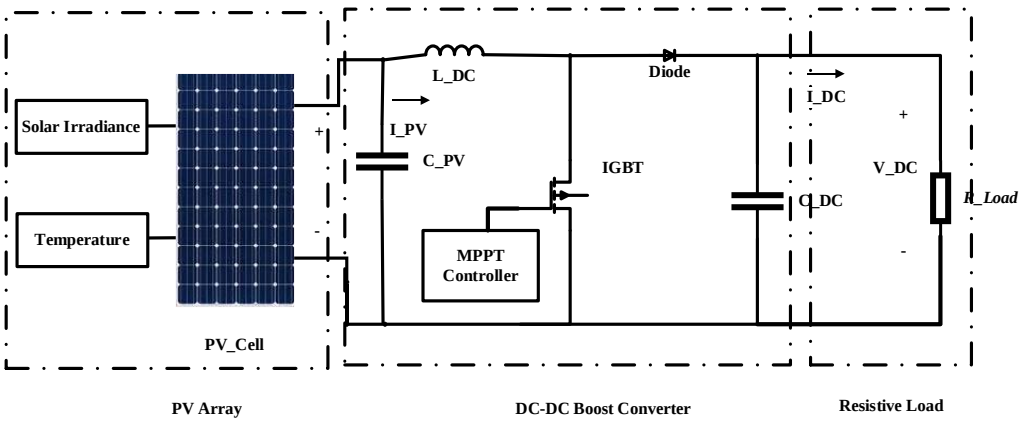

Fig 3.1 Electrical Circuit model of DC-DC Boost Converter

The electrical circuit architecture of the dc-dc boost converter is shown in Fig. 3.1. Inductance, the resistive load, switch frequency, diode PV input, and dc output capacitance filter are all part of it. The inductance and capacitance of the MPPT circuit are determined using the dc-dc inverter architecture. The inductance is determined to keep the MPPT converter running in continuous current mode (CCM). The controller must remain in CCM to ensure constant output. If the inductance is low, the MPPT translator will operate in discontinuous current mode (DCCM). (DCCM). When the inductance is excessively high, the MPPT processor grows and the tracking response is delayed. The capacitance is designed to keep the voltage ripple within the limitations provided. The voltage ripple is too big when the capacitance is too low. When the capacitor grows too big, the MPPT inverters' reaction time becomes sluggish[23]. The mathematical model of the design of the dc-dc boost converter parameters can give by equations (3.1) to (3.4)

$$V_{dc} = \frac{V_{pv}}{1-D} \tag{3.1}$$

$$C_{pv} = \frac{D^2 I_{dc}}{\frac{\Delta V_{dc}}{V_{dc}}(1-D) f_{sw} V_{pv}} \tag{3.2}$$

$$L_{dc} = \frac{V_{pv} D}{\Delta I_{dc} f_{sw}} \tag{3.3}$$

$$C_{dc} = \frac{I_{dc} D}{\Delta V_{dc} f_{sw}} \tag{3.4}$$

Where is:

V_{dc} = DC- output voltage generated from boost converter

V_{pv} = input voltage generated from PV cell

I_{pv} = photovoltaic current

I_{dc} = DC- current generated from boost converter

L_{dc} = dc-dc boost converter inductance

C_{pv} = input capacitor filter

C_{dc} = output capacitor filter

D = duty cycle (0-1)

f_{sw} = switch frequency

ΔV_{dc} = output dc voltage ripple

ΔI_{dc} = input current ripple

R_{load} = Resistive Load

Depending on the opening and closing of the frequency of switching, the dc-dc boost converter will operate in one of two different modes. In the first operation modes the switch device will be operated on $t = 0$ and switched off when the diode is turned off, during the operation period photovoltaic current (I_{pv}) goes through the dc-dc boost inductor (L_{dc}). In the second operation mode, the switch will turn ON at $t = t_{on}$ and turn off at $t = T$ (where; T= switching period and t_{on} = switching time when the device is on). Therefore total power will be stored in the inductor in the first mode and dc-dc boost current and voltage (V_{dc} , I_{dc}) will go through the output capacitor filter (C_{dc}) and resistive load (R_{load}) [24-26]. Fig.3.2 and Fig 3.3 illustrated the first and second operation modes of the dc-dc boost converter.

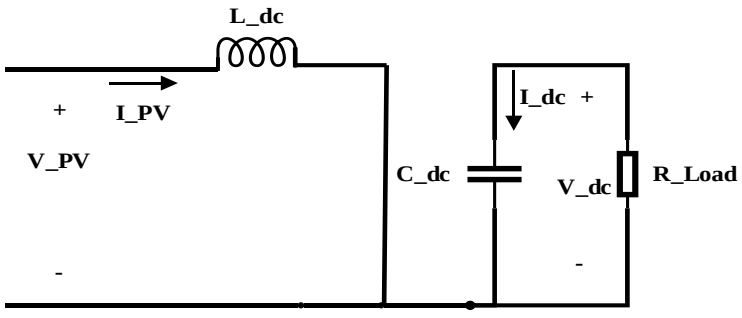

Fig 3.2 First Operation Mode of the Converter

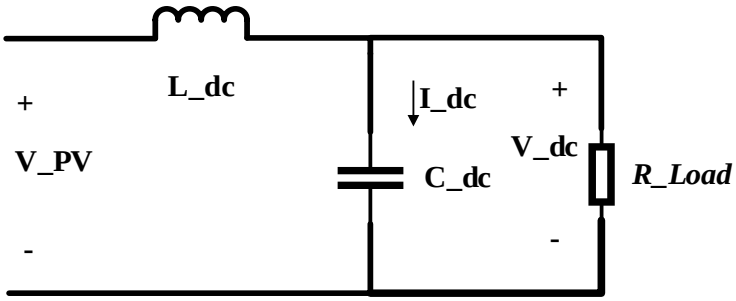

Fig 3.3 Second Operation Mode of the Converter

Table 3.1 shows the specification design parameters of the dc-dc boost converter based on Pulse width Modulation (PWM).

Table 3.1. Design Parameters of Boost Converter

Boost Converter Parameters	Values of the Parameters
Switch Frequency (f_{sw})	$10\,KHZ$
Duty Cycle (D)	0.5
DC-DC Boost Inductance (L_{dc})	$2.795\,mH$
Input PV Capacitor Filter (C_{pv})	$44.71\,\mu F$
Output DC Capacitor Filter (C_{dc})	$0.51413\,\mu F$
Resistive Load (R_{load})	36.4Ω

3.3 Application of MPPT Techniques

The photovoltaic system's nonlinear current and voltage (I, V) characteristics adapt to changing climatic conditions (solar irradiance and temperature). As a consequence, the Predictive control algorithms controller is used to increase the power output by the solar cell to match demand and current variations in the environment. Several MPPT algorithms have been studied and shown to be successful. [27]. They differ in terms of implementation simplicity, sensing parameters, convergence time, cost, capacity to distinguish several local and global MPPs, and applications. Because they need a basic feedback approach and are straightforward to execute, P&O and HC strategies are the most often utilized in MPPT algorithms. The feedback current is used in the

incremental conductance (INC), short-circuit current (SCC), and fractional open-circuit voltage (FOCV) MPPT algorithms [28-29]. Research studies are motivated to increase the architecture as well as the efficiency of traditional MPPT techniques such as proportional integral derivative controller (PID), perturbation and observation (PO), and incremental conductance (IC). Studied a PID MPPT technique to provide variable step size that was modified matching to errors to improve the performance of the P&O Optimization technique The genetic algorithm is used to adjust the PID controller (GA)[30]. The PID control scheme is used to regulate the semiconductor switches in the converter in maximum power point tracking (MPPT) for solar systems. The dearth of controllers in a PV-MPPT system, such as a lag-lead compensator, PID controller, or fuzzy logic controller, leads the power optimization method for solar photovoltaic systems to be sluggish and susceptible to significant steady-state error[31-32]. This technique has been devolved to develop the effectiveness of a photovoltaic energy source under the fast change in atmospheric conditions. It has been defined as one of the most outstanding MPPT approaches, in which it has investigated the dynamic behavior of the P&O MPPT methodology and an INC MPPT algorithm, demonstrating that the efficacy of experimental outcomes is up to 95%, although the INC has limits owing to component noise. This research study proposes an MPPT controller based on intelligent PSO-PID controller approaches to solve the limitations of all of the above-mentioned MPPT methodologies. The capacity to decrease steady-state error, regulate imprecise systems, resilience, and the lack of necessity for correct mathematical expression are all advantages of this method.

3.3.1 PID Controller Based MPPT

The Proportional, Integral, and Derivative (PID) controller was initially introduced in 1939, and it is still the greatest extensively employed controller in procedure control these days. The PID controller is a feedback method of control comprised of three independent controllers: the Proportional Controller, the Integral Controller, and the Derivative Controller (P, I, D), therefore the mathematical model of the PID controller and basic structure are shown in equation (3.5) and Fig 3.4 respectively. The PID controller requires the input error signal to be optimized therefore, depending on the input error signal it’s going to generate control optimal value. These controllers can be represented in a variety of transfer functions. The parallel form, ideal forms, and series

forms of PID structure are commonly used in research and applications represented by (3.6), (3.7), and (3.8), respectively. $u_{PID}(t) = K_p e(t) + K_i \int_0^t e(t)dt + K_d \frac{d}{dt} e(t)$ (3.5)

$$U(s) = K_p + K_i \frac{1}{s} + K_d s \tag{3.6}$$

$$U(s) = K_p \left(1 + \frac{1}{T_i} \times \frac{1}{s} + T_d s \right) \tag{3.7}$$

$$U(s) = K_p \left(1 + \frac{1}{\tau_i} \times \frac{1}{s} \right) (1 + \tau_d s) \tag{3.8}$$

The parallel structure is a typical structure that allows for flexible controller parameter assignment. We can transfer the ideal PID structure to series when $\tau_d \le \frac{\tau_i}{4}$ the steps of converting forms are shown in equation (3.9). In practice, it's frequently used in conjunction with a filter with short time constants. [33-35].

$$K_p = k_p \left(1 + \frac{\tau_d}{\tau_i} \right), T_i = \tau_i \left(1 + \frac{\tau_d}{\tau_i} \right), T_d = \frac{\tau_d}{1 + \tau_d / \tau_i} \tag{3.9}$$

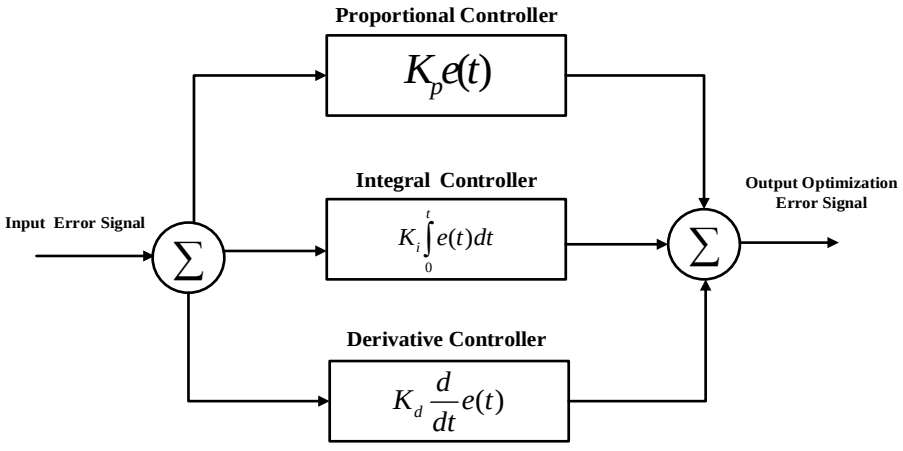

Fig 3.4 Model of PID Controller

3.3.2 Particle Swarm Optimization (PSO) Based MPPT

In 1995, Kennedy and Eberhart presented the particle swarm optimization (PSO) method, This is a swarm intelligence-based intelligent optimization approach. The PSO is a method for population-based evolutionary algorithms. It is simple to implement and has an excellent computing performance as well as a consistent convergence feature. It is not necessary to understand the gradient information of a system's reaction. This new heuristic approach solves continuous nonlinear optimization problems with a high level of reliability. It can produce a high-quality response in a shorter amount of time [37-39]. The hunting behaviors of birds and fish schools inspired the development of this approach, and the research team used this phenomenon to solve heuristic search issues. Several cooperating birds are utilized in this method, so each bird, known as a particle, will have its optimal solution that is represented by an objective function, as well as velocity, that is used to calculate the direction and distance of their movement. Every particle shares information gleaned through its search process [36].

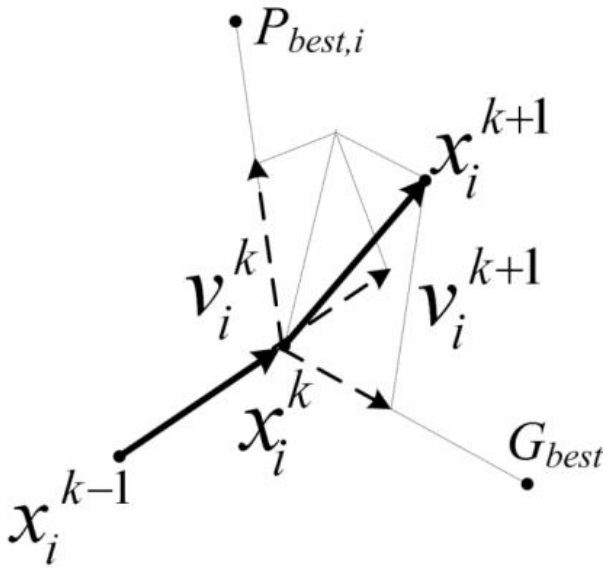

Fig 3.5 Operation Principe of PSO Algorithm

Fig 3.5 represents the behavior of particles swarm optimization which is controlled by various parameters; the P_{best}, which is used to save the best location from each particle as an

independent best position, and the G_{best}, which is discovered by analyzing particle swarm optimization and preserved as the swarm's best possible position. The particle attempts to modify its location utilizing the present position, current velocity, the difference in values between the current position and the previous personal best position, as well as the current position and the previous global best position values. The fitness value assesses particle behavior to see if the finest solution is found and, if not, repeatedly improves the solutions. Iterate this step until the required halting requirement is met an excellent fitness or a maximum number of iterations is usually used as a stopping criterion. The operation sequence of the PSO algorithm is represented by a mathematical model in equations (3.10) and (3.11).

$$v_i(k+1) = wv_i\left(k\right) + c_1 r_1\left(P_{best} - x_i\left(k\right)\right) + c_2 r_2\left(G_{best} - x_i\left(k\right)\right) \tag{3.10}$$

$$x\left(k+1\right) = x_i\left(k\right) + v_i\left(k+1\right) \tag{3.11}$$

Where is

P_{best} is Personal best position

G_{best} is Global best position

w is Inertia weight

c_1 and c_2 learning Factor and social coefficient

r_1 and r_2 are random values in the range of (0 - 1)

v_i is the Velocity of the particle

x_i is the Position of the particle

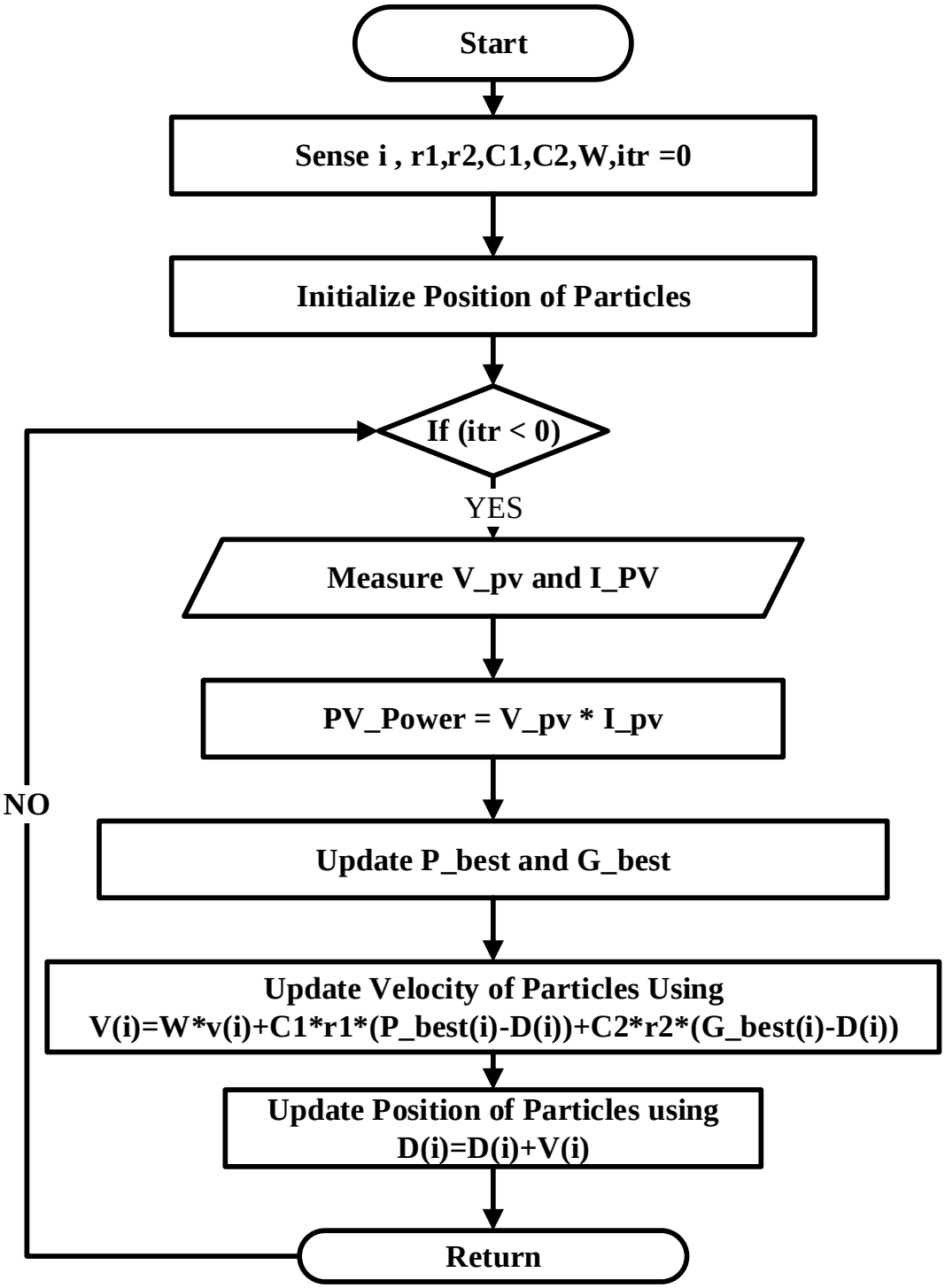

Fig 3.6 Flowchart of PSO algorithm based MPPT

3.3.3 Intelligent PSO-PID Controller-Based MPPT

MPPT techniques use controllers to modify the setpoint of the PV energy generation system to match the generated reference value. There are several variations of MPPT in the literature, each with a unique tracking variable option; therefore, tuning PID controller parameters is critical to get decent system responsiveness. In this work, we have proposed new MPPT techniques based on a hybrid Intelligent PSO-PID Controller. The PID controller variables (K_i , K_p , and K_d) are optimized for maximum power point tracking based on a photovoltaic system utilizing the PSO method. The population space is three-dimensional, with matrices representing location and velocity. In the solution space, every potential set of controller parameter values is given as a particle, and its parameters are modified by minimizing the error. A discrete PID controller will be used to design the MPPT controller. The input error signal depending on the non-linear I-V curve (dV_{pv} , dI_{pv}), is evaluated as shown by equations (3.12),(3.13), and (3.14); therefore, the proposed controller reduces the error signal to zero between dV_{pv} and dI_{pv}. The amount of dV_{pv} and dI_{pv} will be calculated by solar irradiance and temperature.

$$e(t) = \frac{I_{pv}}{V_{pv}} + \frac{dI_{pv}}{dV_{pv}} \tag{3.12}$$

$$dV_{pv} = V_{pv}(t) - V_{pv}(t-1) \tag{3.13}$$

$$dI_{pv} = I_{pv}(t) - I_{pv}(t-1) \tag{3.14}$$

In the case of low errors, the hyperbolic cosine non-linear technique has been presented to give considerable integral regulating effects for big mistakes to limit system settling time and gain, which will reduce oscillations around the MPP. Equations (3.15) and (3.16) represent a mathematical model of the controller. Fig 3.7 illustrates a block diagram of the proposed controller.

$$u_{PID} = K_p + \frac{K_i T_s g(e)}{z-1} + \frac{K_d N_c}{1 + \frac{N_c T_s}{z-1}} \tag{3.15}$$

$$g(e) = \cosh(g_0 e) = 0.5 \times (\exp(g_0 e) + \exp(-g_0 e)) \tag{3.16}$$

$$where; e = \begin{cases} e & ; |e| \le e_{\max} \\ e_{\max}\ \mathrm{sgn}(e) & ; |e| \ge e_{\max} \end{cases}$$

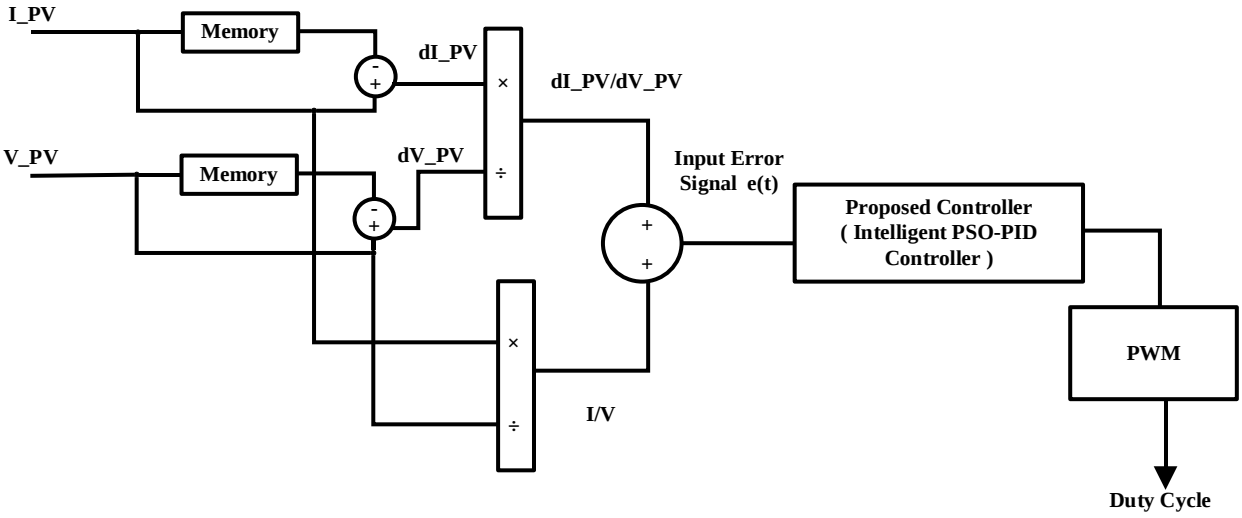

Fig.3.7. Block Diagram of Proposed MPPT Controller

In the search space represented by the matrix, PSO will generate a random swarm of particles. Each particle offers a great solution for PID parameters with values ranging from 0 to 50. Position and velocity of the particle (x_i and v_i) are described by matrices with dimensions of 3xSwarm size in this 3-dimensional issue that provides PID parameters (K_p, K_i, and K_d). The swarm size is the number of particles, with 50 being regarded as a large enough number. The optimal PID parameter value is sent to the PID model to decrease the control error signal and improve the power generation capacity.

The following are the steps for utilizing the PSO algorithm to optimize the parameters of a PID controller:

- Initialize PSO parameters i.e. w, c_1, c_2, Dim, Swarm Size.
- Determine the population swarm of PID controller variables (K_p, K_i, and K_d) in the search space with random swarm and velocity.

- Using equations (3.12), (3.13), and (3.14), compute the optimal solution of the particle swarm and assess the error of each particle (3.14).
- Preserve the value of P_{best} and G_{best}, then Contrast the value of P_{best} which have low error between the current iteration with the old best value of G_{best}.therefore, if the current value of G_{best} then adjusted G_{best} to the value and location of the current particles.
- Update values of particle velocity and particle position using equations (3.10) and (3.11).
- Update the optimal value of PID parameters (K_p, K_i, and K_d).

Fig 3.8 shows the flowchart of the proposed intelligent PSO-PID controller for Maximum power point tracking.

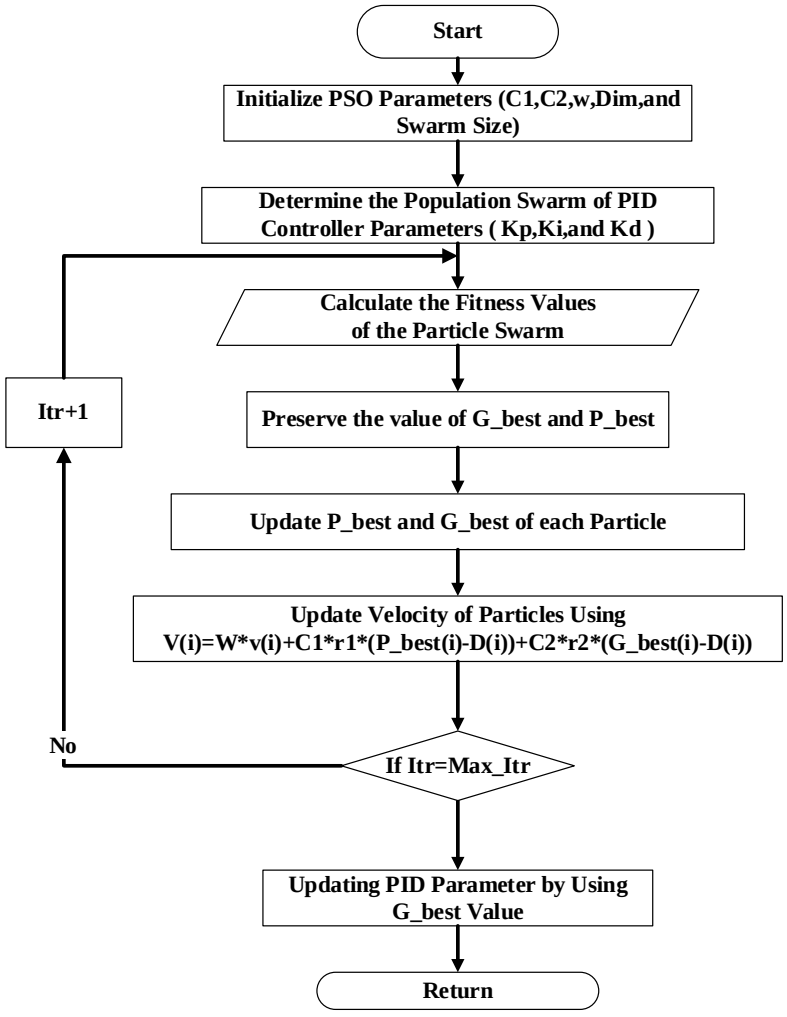

Fig 3.8. Flowchart of Proposed controller based on MPPT

In Fig. 3.1, a photovoltaic system with fixed solar irradiation and temperature. ($1000 W/m^2$ *and* 25^oC respectively) has five PV cells linked in parallel and ten PV cells connected in series which in turn relate to the DC-DC boost converter and resistive load. The PV system was evaluated by using the proposed controller shown in Fig.3.7. Integration of the absolute error over time (IAE) is considered the basic function for reducing the input error signal of the controller to zero, in which positive and negative amounts of input error signal equal to same values. The comparative result of the output power of dc-dc boost converter obtained from simulation using PID, PSO, and Intelligent PSO-PID controller implementing MPPT techniques is illustrated in Fig.3.9 The PSO algorithm generates random PID parameters and optimizes them by choosing the best fitness values which initial values of PID parameters.

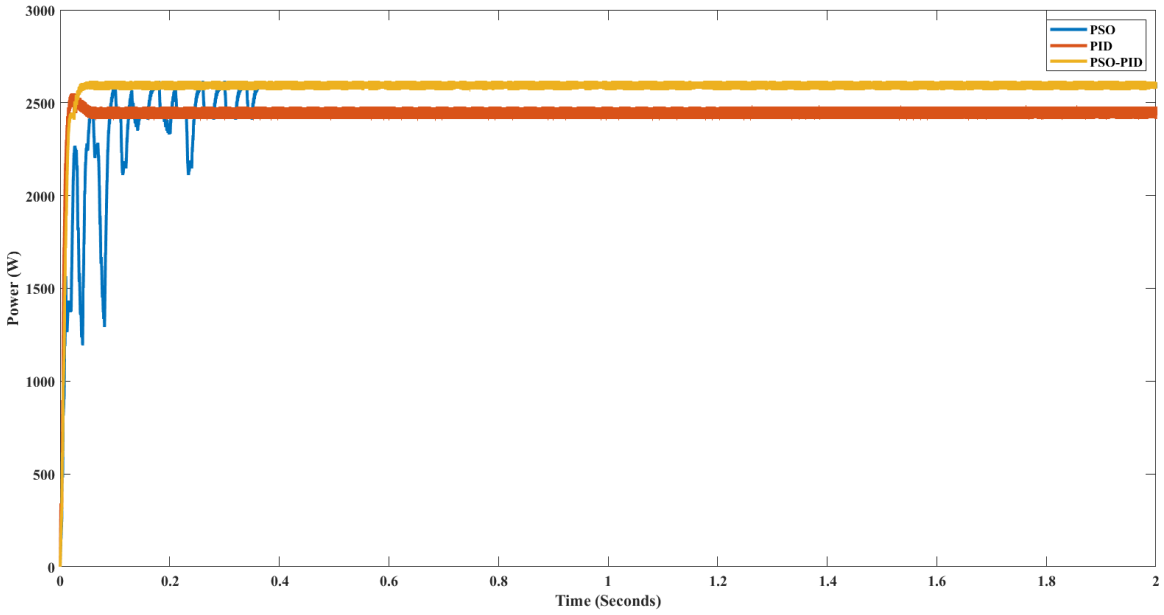

Fig.3.9. Comparison of DC-DC Boost Power

The MATLAB result shows that the proposed controller has better power efficiency in comparison with PID and PSO-based converters. The proposed controller has low power loss during tracking power at maximum operation point, less settling time (0.056 Sec), and low oscillations that are shown in Table 3.2.

Table 3.2 MPPT Characterizes Performance-based different methods

MPPT Technique's	PID Controller	PSO	Proposed Controller
Output DC POWER	2432 W	2550 W	2591W
Power Loss	173.68W	55.68W	14.68W
Power Efficiency	89%	97%	99.4%
Settling Time	0.072 Sec	0.37 Sec	0.056 Sec

CHAPTER 4 DESIGN CONTROLLER FOR SINGLE-PHASE GRID-CONNECTED PV SYSTEM

4.1 Overview

Photovoltaic panels supply direct current (DC) energy to the power electronics components. DC-DC converters are widely used to increase the voltage output of PV cells. Inverters have been used to convert high-level direct current voltage to the alternating current voltage required to power conventional loads. Grid-connected photovoltaic systems are categorized based on the number of output stages. The preceding, single-stage, was applied to the system that used centralized inverter systems. In grid-connected PV systems nowadays, two-step techniques are used, with a dc-dc converter coupled along with the solar module and the dc-ac inverter.

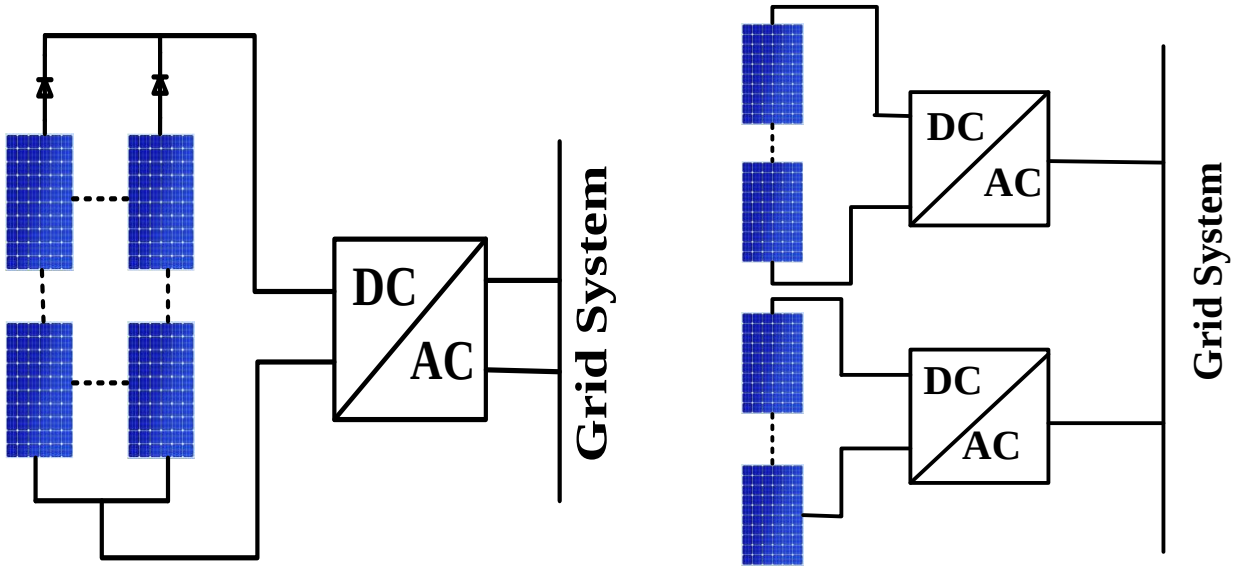

(a) Center Inverter Type (b) Reduced Center Inverter Type

Fig. 4.1 Single Stage configuration

The first generation of grid-connected Photovoltaic systems, seen in Figure 4.1 (a), connect directly a centralized grid-connected DC/AC inverter to an array of Photovoltaic panels. To generate a sufficient voltage output, the Photovoltaic cells are linked in serial, commonly known

as PV strands. To produce high output power, the PV strings are then linked in parallel using string diodes. The centralized DC/AC inverter is subjected to maximum power point tracking (MPPT), grid current regulation, and voltage amplification if essential in this configuration. Therefore, the configuration is simple, and the disadvantages are significant. One of the most significant is the centralized MPPT's insufficient energy collecting abilities as a result of shading, panel mismatches, and deterioration issues [41]. Figure 4.2 (b) shows reduced power variants of the centralized inverter design were created using MPPT for each PV string separately.

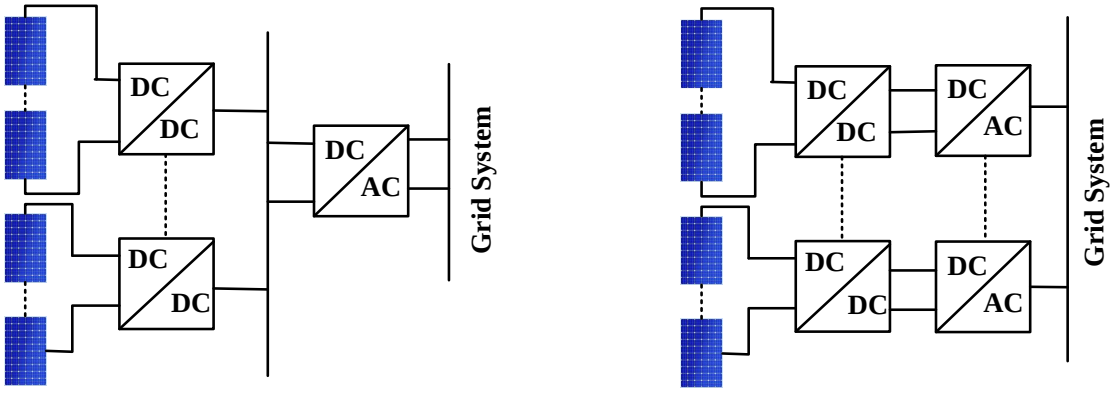

(a) Inverter PCC at AC connected (b) Inverter PCC at DC-AC at the input

Fig 4.2 Double Stage Configuration

Specialized dc converters that conduct MPPT for each solar string can be mounted in the center between the photovoltaic panels and the dc-ac inverter to optimize the energy delivered by the PV cell[42]. As illustrated in figure 4.2, the output of the dc-dc converter can have either a modest cascading effect of the dc voltage or a regulated current that maintains a rectified sinusoidal waveform (a). In the latter scenario, the dc-dc converter maintains the MPPT and output current controller, while the dc-ac inverter adjusts at the system frequency to create the inverted sinusoidal waveform. In figure 4.2, several dc-dc converters feed one inverter topology (b). The MPPT and voltage amplifier is adjusted by the dc-dc converters, while the main dc-ac inverter handles output current control.

4.2 Design Strategy of Proposed System

Figure 1.1 depicts a block schematic of the proposed model, which includes a 2.8 KW photovoltaic array linked to a linear load and power grid system. The suggested system is made

up of a PV cell and a dc-dc boost converter that uses MPPT methods, a full-wave H-bridge with two legs along with a dc-ac inverter type of voltage source inverter (VSI), dc-link capacitor, LCL filter, and linear load. The grid-connected PV system it's become a very important part of the application of photovoltaic systems recently. Generally, two control techniques use to regulate output power produced by PV panel grid-connected systems which are voltage control strategy and current control strategy. If voltage regulation is used to regulate the inverter output, the system is paralleled with two voltage sources. In this scenario, reaching the performance indices is difficult. To achieve PV grid-connected, the grid is thought to be a voltage source with limitless capacity, regulating the output current of the inverter and tracking the phase of the grid voltage [42]. The Phase Lock Loop (PLL) architecture is proposed as a feedback control system to meet grid phase synchronization.

4.2.1 Design Size of DC-Link Capacitor and DC-Link Voltage

The voltage oscillations at the capacitor and dc-link are created by the double line energy utilization traveling between the input of the phase grid and the outside of the phase grid, which is coupled to a photovoltaic system. As a result of the voltage ripple, the heating of the passive components and dc source rises, affecting the MPP performance of PV cells[43]. To go with this issue a capacitor is connected in parallel between dc-dc boost converter and dc-ac inverter, which is directly proportional to both the dc voltage and ripple voltage. Figure 4.3 illustrated the placement of the dc-link capacitor.

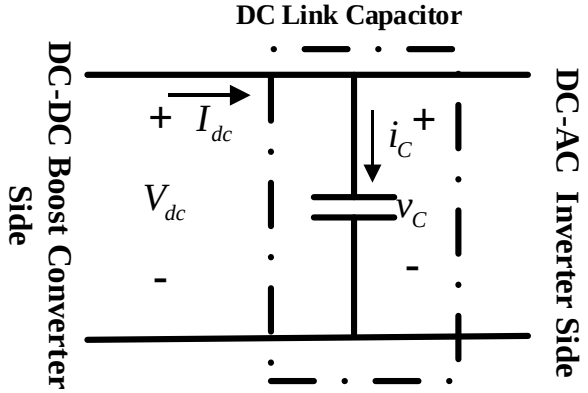

Fig 4.3. Placement of DC-Link Capacitor

The dc-dc boost converter supplies electric power to both the dc-link capacitor and voltage source inverter (VSI) calculated by equations (4.1), (4.2), and (4.3)

$$P_{dc\,converter} = P_{dc\_C} + P_{VSI} \tag{4.1}$$

$$P_{dc\_C} = C_{dc\_Link} V_{dc} \Delta V_{dc} \tag{4.2}$$

The power generated from PV cell to dc-dc boost converter to VSI equal to power grid then,

$$C_{dc\_Link} = \frac{P_{grid}}{4\pi f_{grid} V_{dc} \Delta V_{dc}} \tag{4.3}$$

Where are f_{grid} frequency grid, V_{dc} is dc-link voltage, and ΔV_{dc} is ripple voltage.

The DC-link voltage needs to be more than double the peak phase grid voltage at the common point of interconnection (CPI) [44]. The value of dc-link is calculated by equation (4.4).

$$V_{dc} = \frac{2.83 V_{grid}}{\sqrt{3}\ m} \tag{4.4}$$

Where are V_{grid} is the line of grid voltage and m is the modulation index

Table 4.1 DC-link Capacitor size in the different ripple voltage

Grid Power (P_{grid})	Grid Frequency (f_{grid})	DC Link Voltage (V_{dc})	DC Ripple Voltage (ΔV_{dc})	Capacitor size (C_{dc_Link})
$2.6\,KW$	$50\,HZ$	376 V	$7.52\ at\ 3\%$	$975.66\ \mu F$
$2.6\,KW$	$50\,HZ$	376 V	$18.8\,at\,5\%$	$585.39\,\mu F$
$2.6\,KW$	$50\,HZ$	376 V	$31.96\,at\,8.5\%$	$344.35\,\mu F$

Table 4.1 shows the different levels of dc ripple voltage in the rate of KVA of inverter and normal voltage. The size of the dc-link capacitor is designed at dc ripple voltage (ΔV_{dc}) at 8.5 % of dc-

link voltage, dc-link voltage (V_{dc}) at 375.8 V we select 376V, and grid frequency (f_{grid}) at 50 HZ. As a result, the dc-link capacitor value estimated by equation (4.3)is (C_{dc_Link}) $344.35\,\mu F$

4.2.2 Design of LCL Ripple Filter

LCL filters are commonly employed in the application of grid-connected photovoltaic systems to obtain reduced unwanted voltage, current, and frequency harmonics. The LCL filter is a third-order filter characterized by reactive elements, with a rating of dampening 60db/dec. The LCL filter in this work was developed using a current ripple approach to acquire optimum reactive control parameters and damping resistance. The IEC 61000-3-2 standard is used to assess the overall grid stability of harmonic current. Therefore, it consists of damping resistance ($R_{damping}$), inverter inductance (L_{inv}), grid inductance (L_{grid}), and capacitor filter (C_{filter}) which are illustrated in figure 4.4. The mathematical model of the LCL filter is represented by equations (4.5) to (4.13).

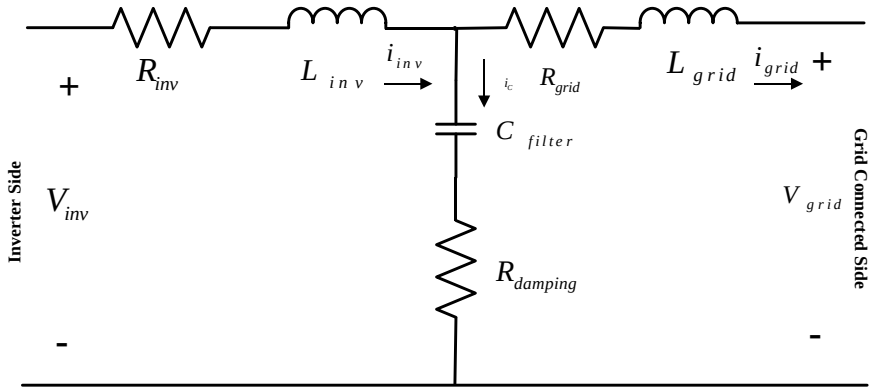

Fig 4.4. Electric Model of LCL Filter

$$G(s) = \frac{I_{grid}(s)}{V_{inv}(S)} \tag{4.5}$$

$$G(S) == \frac{R_{damping}C_{filter}s + 1}{L_{inv}L_{grid}C_{filter}s^3 + (L_{inv} + L_{grid})R_{damping}C_{filter}s^2 + (L_{inv} + L_{grid})^2} \tag{4.6}$$

By ignoring damping resistance;

$$G(s) = \frac{1}{1+(\frac{s}{\omega_{res}})^2(L_{inv}+L_{grid})s} \tag{4.7}$$

$$I_{ripple} = \frac{V_{inv}}{8L_{inv}f_{sw}} \tag{4.8}$$

$$\omega_{res} = \sqrt{\frac{L_{inv}+L_{grid}}{L_{inv}L_{grid}C_{filter}}} \tag{4.9}$$

$$C_{filter} = \frac{\alpha P_{grid}}{2\pi f_{grid}V_{grid}^2} \tag{4.10}$$

$$L_{inv} = \frac{V_{imv}}{8f_{sw}I_{ripple}} \tag{4.11}$$

$$L_{grid} = rL_{inv} \tag{4.12}$$

$$R_{damping} = \frac{1}{3\omega_{res}C_{filter}} \tag{4.13}$$

Where are; ω_{res} is resonance frequency, I_{ripple} is maximum ripple current, α the absorption rate of reactive power in the condition of resonance frequency, and r is the factor between inverter inductance and grid inductance. The LCL filter parameters are designed as $r = 0.6$, grid frequency (f_{grid}) at 50 HZ, switch frequency f_{sw} is 10 kHz, and $\alpha\, at\, 5\%$. Therefore, the values of LCL filter parameters calculated by questions (4.10), (4.11), (4.12), and (4.13) are $R_{damping} = 2.8056\Omega$, $C_{filter} = 7.8224\,\mu F$, L_{inv} =1.5mH , and $L_{grid} = 0.88667\ mH$.

4.2.3 Single Phase Lock Loop (PLL) based Transport Delay

Figure 4.5 depicts the phase lock loop's three components: a Phase Detector (PD), a Loop Filter (LP), and a Voltage Control Oscillator (VCO). The VCO produces the resulting oscillations, The PD module, on the other hand, computes the phase shift of the input and output signals, also known as the phase difference between input and output. The Loop Filter, which is commonly a PI controller, is used to reduce phase error and deliver an appropriate controlling signal to the

VCO. The application of SRF-PLL serval techniques such as Transport Delay, Inverse Park Transformation, Second Order Generalized Integrators (SOGI), and Hilbert Transformation has been applied to the synchronous phase in the utility grid. In this paper, Single Phase Lock Loop-based Transport Delay method has been proposed for the synchronous phase in a PV grid-connected system [45][46]. Its operation is based on resetting the direct component of the rotating cycle to zero. This technique uses the input voltage V_{grid} as α a factor in $\alpha\beta$ the system, and β the portion may be created simply by adding a phase shift about the input voltage fundamental frequency. As a result, to diagnose phase errors, the Park Transform can be employed., which is represented by (4.14). This component is derived using the predicted phase angle.

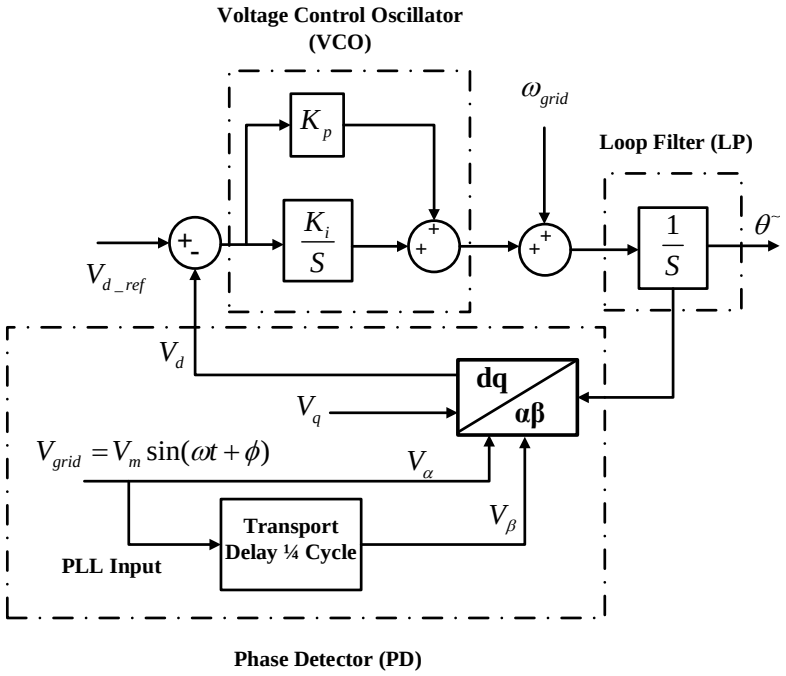

Fig. 4.5 Block Diagram of SRF-PLL based Transport Delay

$$\begin{bmatrix} V_d \\ V_q \end{bmatrix} = \begin{bmatrix} \cos\theta^{\sim} & \sin\theta^{\sim} \\ -\sin\theta^{\sim} & \cos\theta^{\sim} \end{bmatrix} \begin{bmatrix} V_{grid} \\ V_\beta \end{bmatrix} = \begin{bmatrix} V_{\max}\sin(\Delta\theta) \\ -V_{\max}\cos(\Delta\theta) \end{bmatrix} = \begin{bmatrix} V_{\max}\Delta\theta \\ -V_{\max} \end{bmatrix} \quad (4.14)$$

4.2.4 Control Strategy of VSI Voltage

The purpose of controlling VSI voltage is to regulate the amount of the sinusoidal waveform grid current (I_{grid_ref}), that is in phase along the voltage grid (V_{grid}). The current phase (I_{grid_ref}) represents the active component element of the reference current grid (I_{grid}) [47]. The power from the VSI at the DC side is delivered to the utility grid by precisely controlling the current magnitude and employing a fast grid current controller. The single-phase control strategy approach allows the active and reactive power of a grid-connected solar system to be controlled independently. The single-phase VSI use is to maintain a stable ac-link voltage value and to supply active power into the grid using the decoupling control strategy paradigm. As a result, the power balance is established at the DC-link, causing (V_{dc}) to stabilize at the appropriate level. The fraction order hybrid fuzzy logic PI controller as shown in figure 12 contains a fuzzy logic controller (FLC) and fraction order propositional integral controller (PI). Where, K_e and K_c is input fraction order factor K_{PI} is output factor. Equation (4.15) describes the output signal of the proposed Controller. Peak power stability concepts may be used to compute the mathematical relationship between the dc-average link's voltage and fluctuations in the amount of the basic grid current while neglecting converter losses. The fuzzy logic rule-based is shown in Table 4.2.

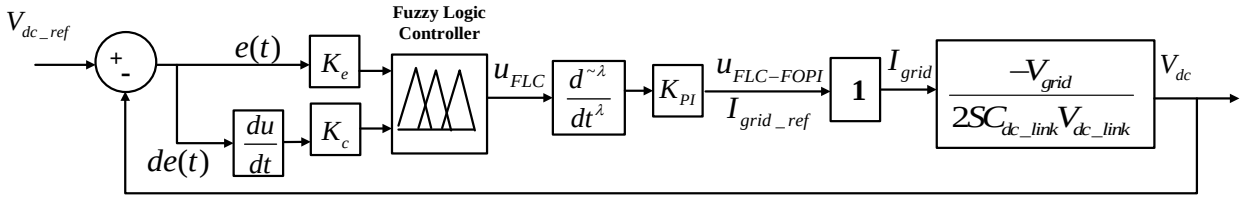

Fig.4.6 Structure of Proposed Controller

$$u_{FLC-FOPI} = K_{PI}\frac{d^{-\lambda}u_{FLC}(t)}{dt^{-\lambda}} \tag{4.15}$$

$$P_{dc} = P_{grid} + P_{dc\_C} \tag{4.16}$$

$$\frac{dC_{dc\_link}V_{dc\_link}^2}{2dt} = -\frac{V_{grid}I_{grid}}{2} \tag{4.17}$$

$$\frac{V_{dc}(s)}{I_{grid}(s)} = -\frac{V_{grid}}{2SC_{dc\_link}V_{dc\_link}} \tag{4.18}$$

Table 4.2 Fuzzy Logic Rules

$\frac{d^{\lambda}e(t)}{dt^{\lambda}}$	$e(t)$						
	LN	MN	SN	Z	SP	MP	LP
LP	LN	MP	LP	SP	Z	MP	LN
MP	MN	MP	SP	Z	SN	SP	SN
MP	SN	SP	SP	SN	MN	Z	Z
MP	Z	Z	SP	MN	MN	SN	Z
SP	SP	SN	Z	MN	LN	SN	Z
Z	MP	MN	SN	MN	LN	MN	LN
SN	LP	MN	MN	LN	LN	LN	MN

4.2.5 Control Strategy of VSI Current

The current regulation is used to create superior power quality and performance, which are both crucial for achieving regulatory requirements. An internal current regulator's dynamic reaction is often quicker than that of an external voltage controller. The voltage source inverter (VSI) must provide a sinusoidal grid current with a decrease in the rate of THD and a power factor around unity. As a consequence, the amount of the reference grid current is increased by a sinusoidal reference frame produced from a grid-synchronized phase-locked loop (PLL). The grid current is then forced to conform to this sinusoidal standard by the internal current loop regulator. A block schematic of the control strategy loop-based grid voltage feedforward is shown in Figure 4.7.

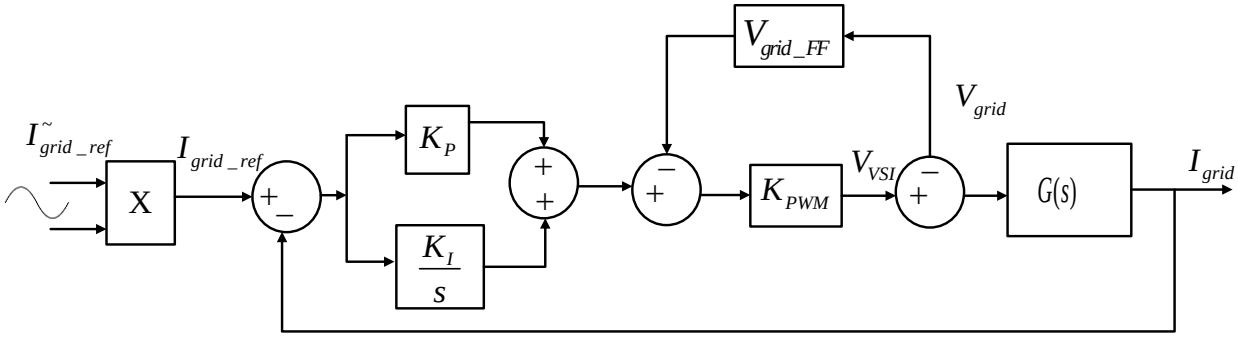

Fig 4.7. Block Diagram of VSI Current Control Loop Based Grid Voltage Feedforward

The reference current of the grid I_{grid_ref} is compared with the measured grid current I_{grid} and to reduce steady-state oscillations, the difference is routed through a controller. The preceding controller can eliminate phase angle steady-state oscillation without using the voltage feedforward, and it can also reject disturbances. Equations (4.19) and (4.20) express the miasmatical model of the current controller.

$$G(s) = \frac{i_d(s)}{v_d(s)} = \frac{i_q(s)}{v_q(s)} = \frac{1}{R_{grid} + L_{grid}S} \tag{4.19}$$

$$V_{grid\_FF} = \frac{V_{tri}}{V_{dc}} \tag{4.20}$$

CHAPTER 5 RESULTS & DISCUSSIONS

Figure 5.1 represents the proposed molding system which was built by MATLAB Simulink (R 2021b). The proposed system contains a photovoltaic system, DC-DC Converter (Boost Converter) controlled MPPT algorithm, DC-AC inverter (Voltage Source Inverter), DC link Capacitor, LCL filter, and single-phase utility grid with the nonlinear and linear load.

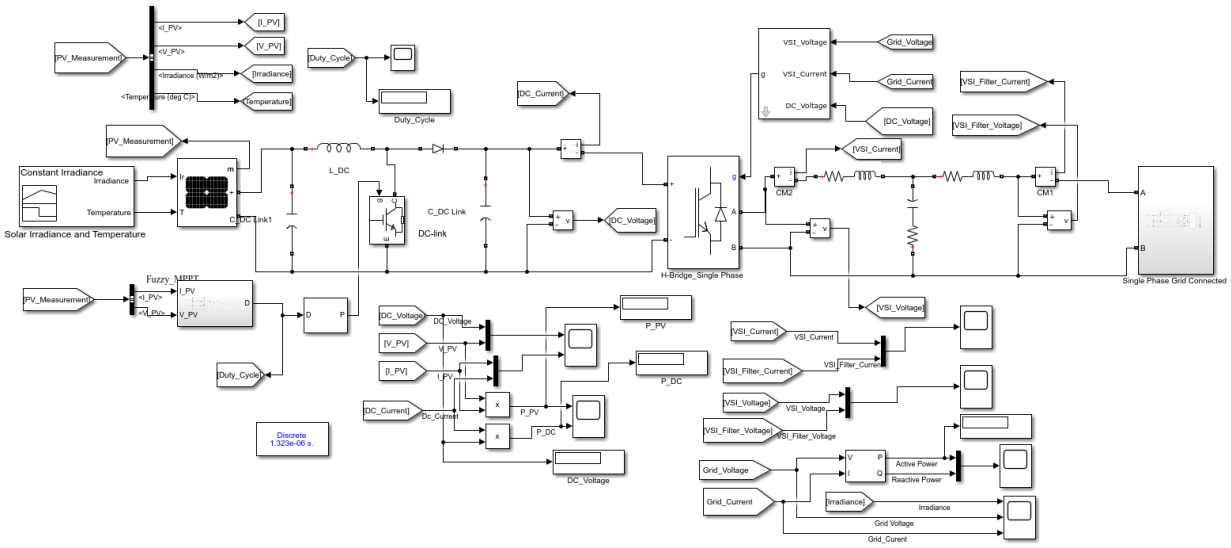

Fig 5.1. Simulation Model of Proposed System

5.1 Results & Discussions

All simulations performed in this work, which illustrate the findings for grid voltage, gird, dc-link voltage, active power, and reactive powers on the AC side provided to the grid system, were completed using the MATLAB/Simulink program. The proposed system in figure 5.1 consists of a PV panel (two Parallel strings and ten Series-connected modules per string), DC-DC Boost Converter controlled by Maximum Power Point Tracking Techniques (MPPT), DC-Link Capacitor, Voltage Source Inverter (VSI), Non-Linear and Linear Load, Single Phase Grid System which has the rate of grid voltage at ($V_{grid} = 330$), grid power ($P_{grid} = 2.8KW$), and grid frequency at ($f_{grid} = 50HZ$). Therefore, simulation results are generated to validate the dependability, accuracy, appropriateness, and efficiency of a proposed system. Furthermore, to validate the efficacy and dependability of a proposed controller, these have been carried out using MATLAB/Simulink scope power system in the different operating conditions of constant solar

irradiation, ramp up / down solar irradiation, step solar irradiation, and constant temperature which illustrated in figure 5.2. Table 5.1 shows the main parameters of the VSI proposed controller, MPPT Proposed Controller (Intelligent PSO-PID Controller), and PI controller. The gain parameters of the Proposed MPPT Controller are optimized by the Particle Swarm Optimization Algorithm (PSO); $\omega = 0.1, C_1 = 1.2,\ C_2 = 2,\ Dim = 3$ .Therefore, the optimization cure of searching optimal parameters of PID controller is illustrated in Figures 5.3,5.4,5.5, and 5.6 respectively. The LCL filter is connected between input VSI and input of grid which aims to reduce unwanted oscillation in grid current and voltage.

Table 5.1 Gain Parameters of Proposed Controllers

Controller	Gain Parameters					
	K_p	K_I	K_D	K_e	K_d	λ
MPPT Proposed Controller	94.41	87.95	14.22	-	-	-
VSI PI Controller	0.6	7.6	-	-	-	-
VSI Proposed Controller	4	100	-	1.5	-0.5	0.9

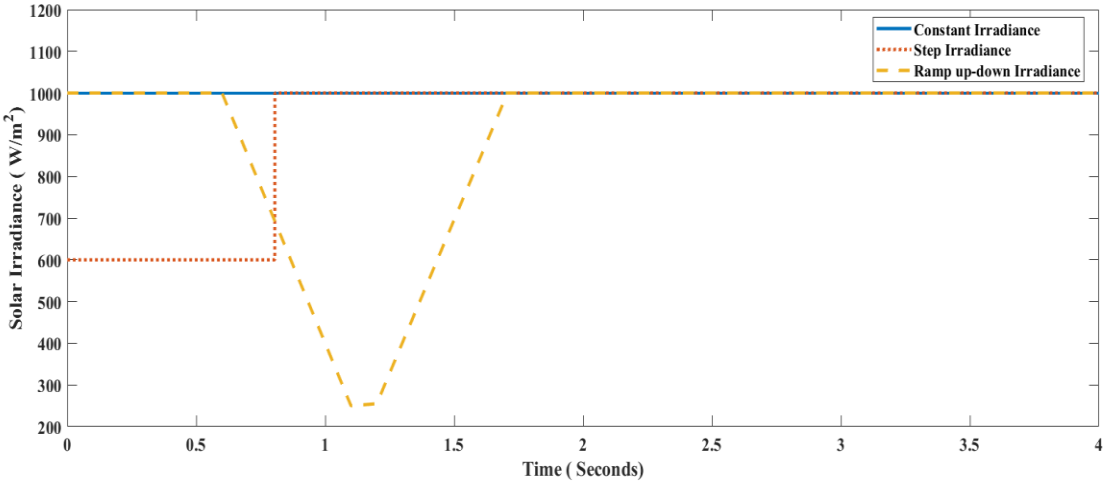

Fig.5.2 Different Operation Tests of Solar Irradiance

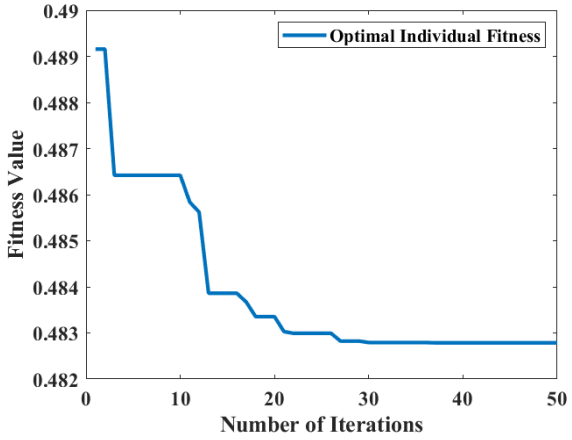

Fig.5.3. Optimal Individual Fitness Curve

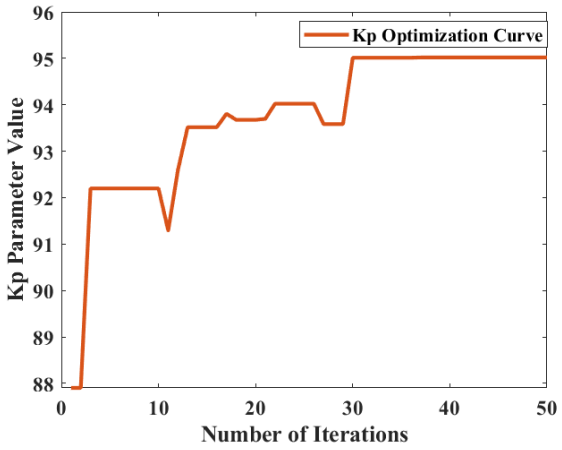

Fig.5.4. K_p Optimization Curve

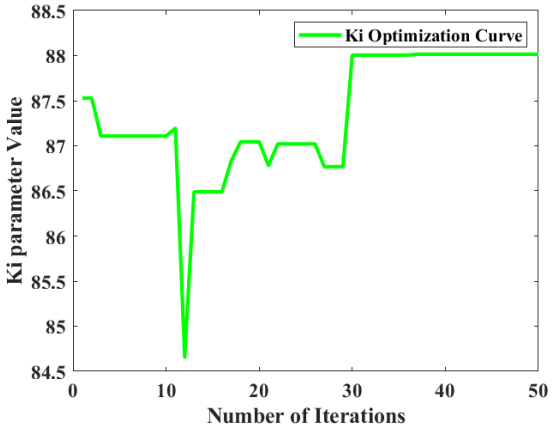

Fig.5.5. K_i Optimization Curve

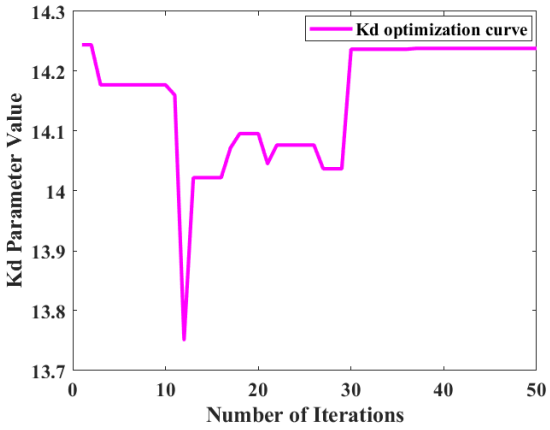

Fig.5.6. K_d Optimization Curve

A. First Seniors: Constant Solar Irradiance and Temperature

In this senior the environmental work of solar irradiance at $1000W/m^2$ and temperature at $25C^o$, the obtaining result of the proposed strategy comparted with Proportional Integral Controller (PI Controller) and optimal parameters of Intelligent PSO-PID Controller optimized by PSO algorithm to get optimal of tracking power produced by PV cell at MPP. Figure 5.7 shows the performance stability of dc-link voltage, the proposed strategy has fast voltage stability at 0.3 sec compared with the PI controller.

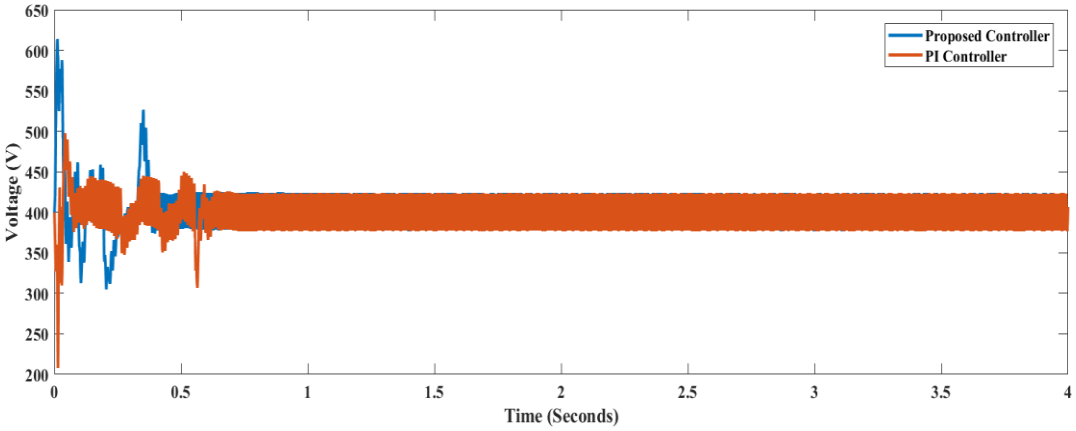

Fig 5.7. DC-Link Voltage

As observed in Figure 5.8, the output voltage and current of the LCL filter reduced oscillation around the current and voltage waveform. Compered the obtained output current and voltage result of VSI with LCL filter and input current and voltage result VSI without LCL, the LCL adjusted output voltage and current at adjustable value and reduced ripple current and voltage to zero. The propped controller has a better tracking reference current and voltage and fast settling time (0.25) compared with the PI controller.

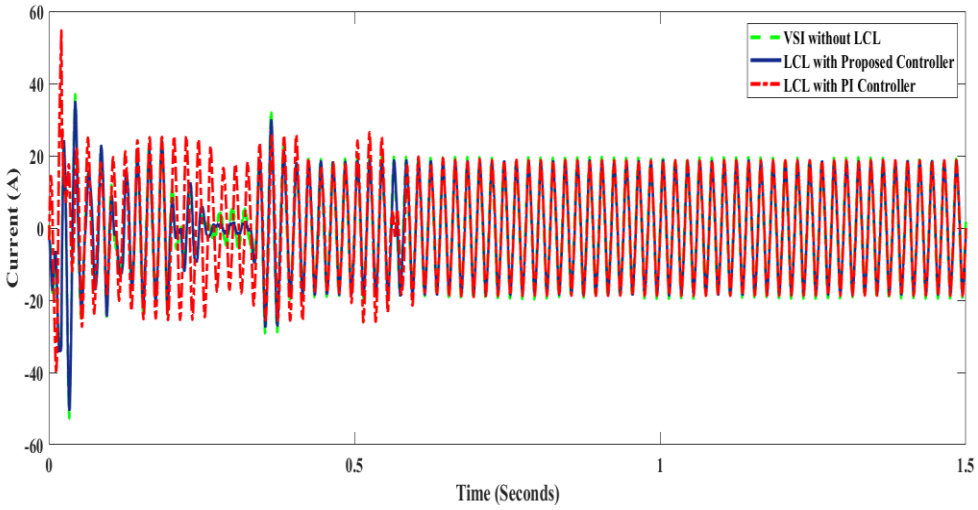

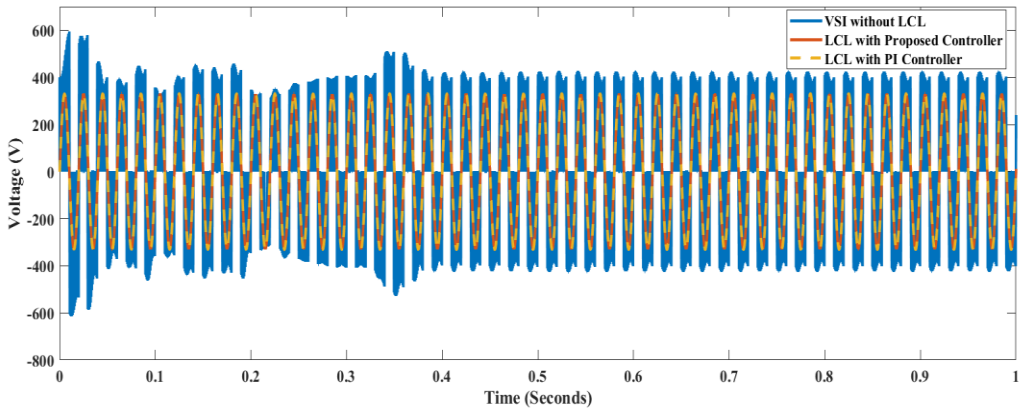

Fig 5.8. Input and Output of LCL filter for VSI Current and VSI Voltage

Figure 5.9 shows the performance of grid voltage and grid current respectively controlled by the suggestion controller and PI controller. From obtained results, it's so obvious the grid current and voltage reach adjusted values with less settling time and oscillation reduced. The performance of active and reactive power of the single-phase grid system is shown in Figure 5.10. The proposed PV panel was injured by constant solar irradiance and temperature, and the output power produced by the PV panel controller by the proposed MPPT achieve optimum tracking at the MPP operation point. The dynamic performance of active and reactive power controlled by the proposed VSI controller has better dynamic performance compared to the PI controller, which reduced overshooting, settling (0.3 sec) time, and steady-state error during tracking power. the reactive maintenance to zero at 0.6 which is faster than the PI controller.

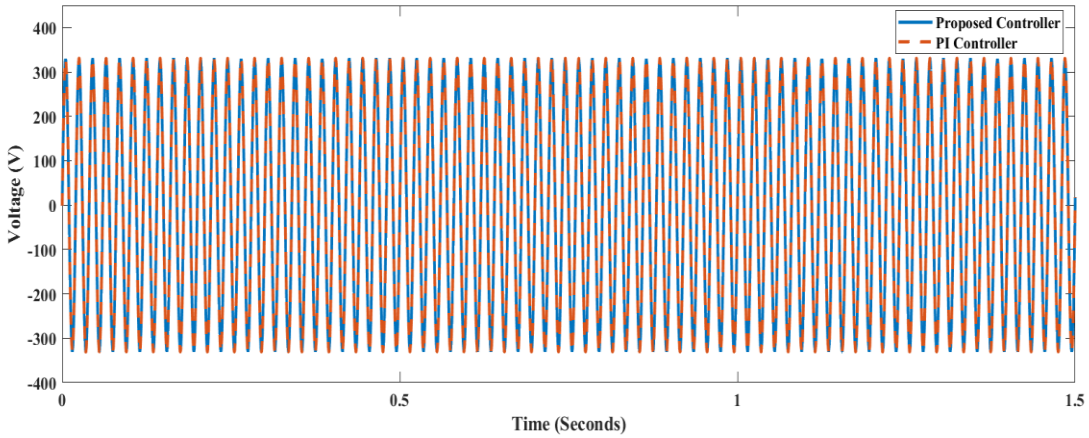

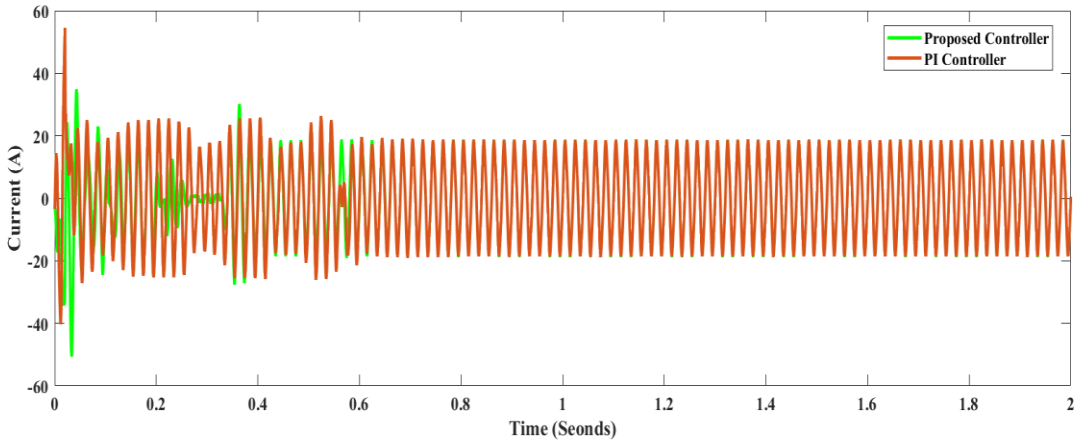

Fig 5.9. Grid Voltage and Grid Current of Single-Phase System

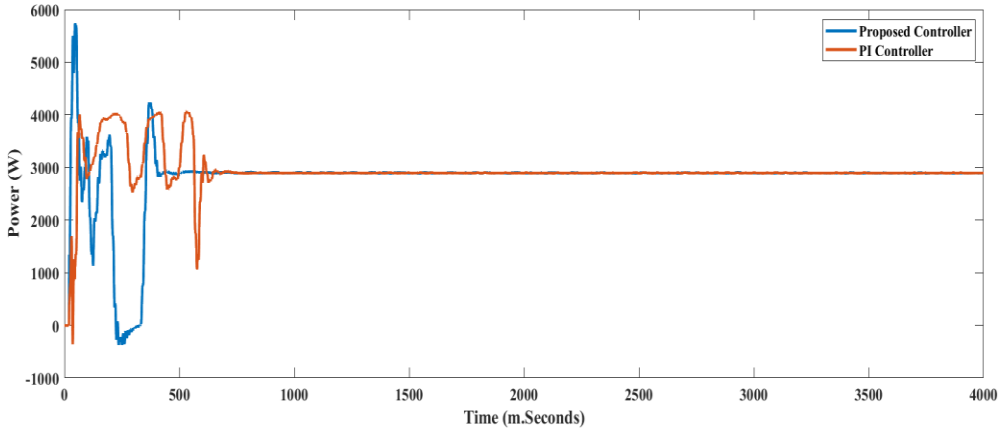

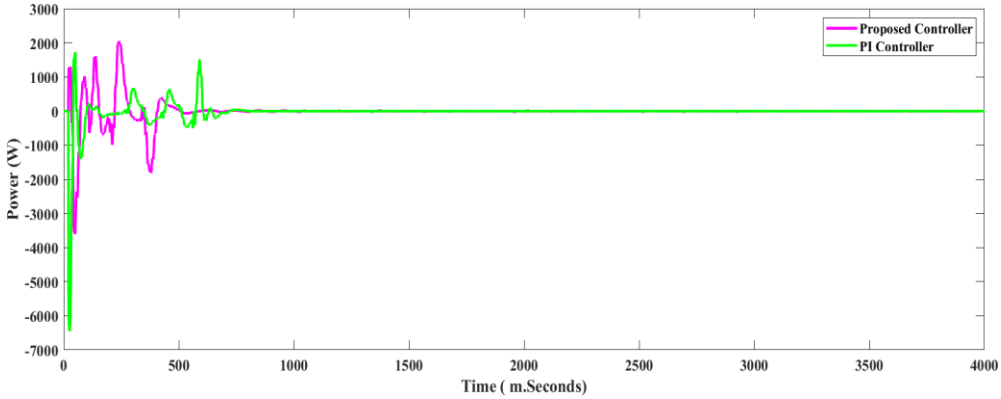

Fig 5.10. Active and Reactive Power of Proposed System with Constant Irradiance

B. Second Seniors: Step Solar Irradiance and Constant Temperature

In this senior, the environmental work of solar irradiance starts with $600W/m^2$, 0.8sec solar change to $1000W/m^2$ and temperature constant $25C^o$ during traveling solar irradiance. Figure 5.11 shows the dynamic performance of active and reactive power of a single-phase grid connect system, the PV penal injected with step solar irradiance, and constant temperature which is shown in Figure 5.2. The proposed controller tracks active power during solar irradiance travel at (0.1 sec), PI controller (1.9 sec) which lost power during the straitly period, and reactive power adjusted to zero for the proposed controller at 0.5 which is faster than the PI controller.

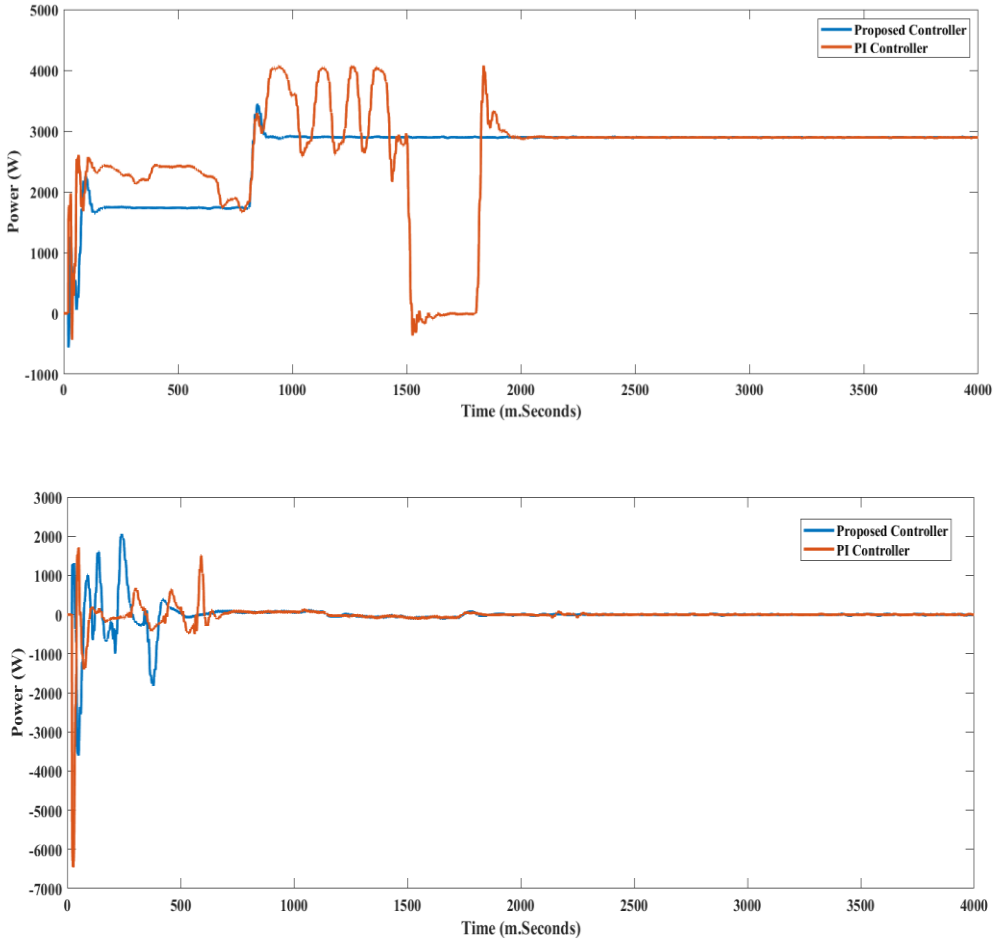

Fig 5.11. Active and Reactive Power of Proposed System with Step Irradiance

C. Third Seniors: Ramp UP-Down Solar Irradiance and Constant Temperature

In this senior, the environmental work of solar irradiance starts with $1000W/m^2$ then start ramping down $0.6\,\text{sec}$ until 1.1sec to $250W/m^2$ at $1.3\,\text{sec}$, solar irradiance start ramping to $1000W/m^2$ at $1.7\,\text{sec}$ during the traveling period of solar irradiance temperature is constant at $25C^o$. Figure 5.12 shows the dynamic performance of active and reactive power of a single-phase grid connect system, the PV penal injected with Ramp Up/Down solar irradiance, and constant temperature which is shown in Figure 5.2. The proposed controller tracks active power during solar irradiance travel at (0.3 sec), PI controller (2 sec) which lost power during the tracking period, and reactive power adjusted to zero for the proposed controller at 0.4 which is faster than the PI controller.

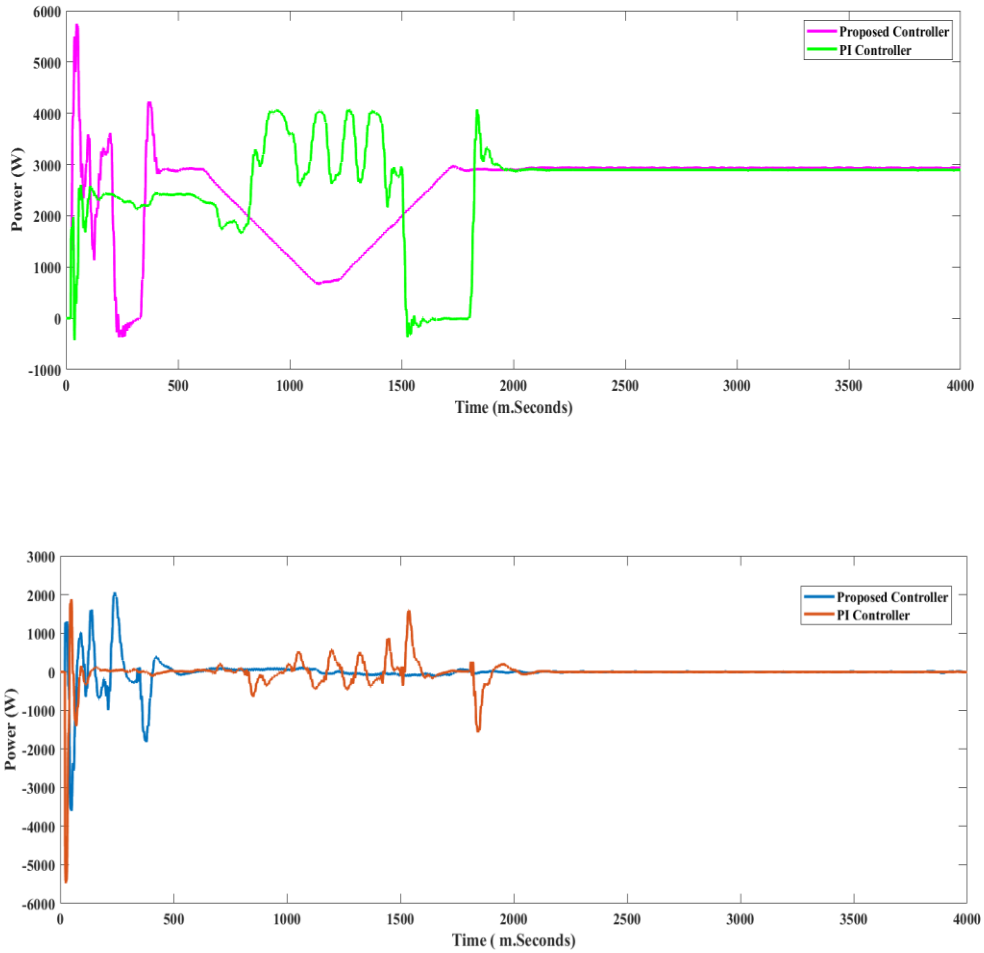

Fig 5.12. Active and Reactive Power of Proposed System with Ramp Up/Down Irradiance

Table 5.2 Comparative analysis of the proposed system in terms of settling time

Solar Irradiance	Stelling Time of Active Power		Stelling Time of Reactive	
	Proposed Controller	PI Controller	Proposed Controller	PI Controller
Constant Irradiance	0.3	0.7	0.5	0.8
Step Irradiance	0.9	1.9	0.6	0.8
Ramp Up-Down Irradiance	1.7	2.3	0.5	2.3

5.2 CONCLUSION

This study has finished the design controller approach of a single-phase grid-connected system-based photovoltaic system. Two controllers are proposed in the system, Intelligent PSO-PID Controller for MPPT techniques and the Hybrid Fuzzy Logic- Fraction Order PI Controller (hFLCFOPI Controller) for control voltage and current in Voltage Source Inverter (VSI). The MPPT strategy is used to verify the operation of the Photovoltaic cell at MPP even in the presence of erratic environmental circumstances. The external voltage control loop regulates the dc-link voltage and injects sinusoidal current into the grid with a low THD. Harmonic distortion does not leak through to the grid current because the dc-link voltage is stabilized and the grid current is managed promptly. To synchronize the phase of the PV-VSI with the energy system, a single-phase lock loop (PLL)-based transport delay mechanism was used, and an LCL filter was used to avoid unwanted ripple in grid current and voltage and eliminate frequency harmonics.

5.3 FUTURE WORKS

There are certain possibilities of the proposed ways for implementing photovoltaic energy sources that can obtain better results; nonetheless, many challenges and intriguing characteristics must be submitted to future studies. The following are some intriguing ideas for further research:

1- Managements active and reactive power photovoltaic system for three-phase grid-connected system.
2- Integral develop grid system on the with battery storage which can supply grid connection at night.
3- Design and optimization protection system of photovoltaic grid-connected system equipment.
4- Investigate the power loss distribution that is impacting the thermal behavior. Hence, the photovoltaic inverter lifetime is challenged.
5- Implements artificial intelligent techniques for controlling and optimizing dc-link voltage and maintains unity power factor.

5.4 PUBLICATION

[1] Mustafa Eltigani I. M, Uma Nangia, Intelligent PSO-PID Controller-Based Maximum Power Point Tracking (MPPT) for Photovoice System, Third International Virtual Conference on Power Engineering Computing and Control (PECCON'22) IEEE-Sponsored.

[2] Mustafa Eltigani I. M, Uma Nangia, Fractional Order Fuzzy Logic Based MPPT Controller for the Photovoltaic System, National Conference on Emerging Trends in Electric - Mobility & Sustainable Development: Opportunities & Challenges (NCETEMSD-2K22).

[3] Mustafa Eltigani I. M, Uma Nangia, and Gomaa Haroun A.H, "Application of ADRC And PID Controller to Distributed LFC For an Interconnected Multi-Area Power System," IJESRT, vol. 10, no. 8, pp. 10–25, Aug. 2021.

[4] Mustafa Eltigani I. M, Uma Nangia, and Gomaa Haroun A.H, "Modeling and Simulation of an Interconnected Multi-Area Thermal Power System Using hFLPID Controller Based Optimization Technique," IAR Journal of Engineering and Technology, vol. 2, no. 5, pp. 22–35, Oct. 2021.

5.5 REFERENCES

[1] R. Sabzehgar, "A review of AC/DC microgrid-developments, technologies, and challenges," 2015 IEEE Green Energy and Systems Conference (IGESC), Nov. 2015, doi: 10.1109/igesc.2015.7359384.

[2] S.M. Mirhassani, S. Z. M. Golroodbari, S. M. M. Golroodbari, and S. Mekhilef, "An improved particle swarm optimization based maximum power point tracking strategy with variable sampling time," International Journal of Electrical Power & Energy Systems, vol. 64, pp. 761–770, Jan. 2015, doi: 10.1016/j.ijepes.2014.07.074.

[3] P. K. Bonthagorla and S. Mikkili, "A Novel Fixed PV Array Configuration for Harvesting Maximum Power from Shaded Modules by Reducing the Number of Cross-Ties," IEEE Journal of Emerging and Selected Topics in Power Electronics, vol. 9, no. 2, pp. 2109–2121, Apr. 2021, doi: 10.1109/jestpe.2020.2979632.

[4] K. Ishaque, Z. Salam, and Syafaruddin, "A comprehensive MATLAB Simulink PV system simulator with partial shading capability based on two-diode model," Solar Energy, vol. 85, no. 9, pp. 2217–2227, Sep. 2011, doi: 10.1016/j.solener.2011.06.008.

[5] M. Kermadi and E. M. Berkouk, "Artificial intelligence-based maximum power point tracking controllers for Photovoltaic systems: Comparative study," Renewable and Sustainable Energy Reviews, vol. 69, pp. 369–386, Mar. 2017, doi: 10.1016/j.rser.2016.11.125.

[6] M. Y. Ye and S. Li, "Simulation Study of PFC Boost Converter Based on Predicted Average Current Control," Advanced Materials Research, vol. 462, pp. 738–742, Feb. 2012, doi: 10.4028/www.scientific.net/amr.462.738.

[7] T. Esram and P. L. Chapman, "Comparison of Photovoltaic Array Maximum Power Point Tracking Techniques," IEEE Transactions on Energy Conversion, vol. 22, no. 2, pp. 439–449, Jun. 2007, doi: 10.1109/tec.2006.874230.

[8] F. Blaabjerg, R. Teodorescu, M. Liserre, and A. V. Timbus, "Overview of Control and Grid Synchronization for Distributed Power Generation Systems," IEEE Transactions on Industrial Electronics, vol. 53, no. 5, pp. 1398–1409, Oct. 2006, doi: 10.1109/tie.2006.881997.

[9] Heinrich Häberlin, Photovoltaics : system design and practice. Hoboken, Nj: John Wiley & Sons Ltd, 2012.

[10] W. Xiao, F. F. Edwin, G. Spagnuolo, and J. Jatskevich, “Efficient Approaches for Modeling and Simulating Photovoltaic Power Systems,” IEEE Journal of Photovoltaics, vol. 3, no. 1, pp. 500–508, Jan. 2013, doi: 10.1109/jphotov.2012.2226435.

[11] E. A. Silva, F. Bradaschia, M. C. Cavalcanti, and A. J. Nascimento, “Parameter Estimation Method to Improve the Accuracy of Photovoltaic Electrical Model,” IEEE Journal of Photovoltaics, vol. 6, no. 1, pp. 278–285, Jan. 2016, doi: 10.1109/jphotov.2015.2483369.

[12] B. K. Nayak, A. Mohapatra and K. B. Mohanty, "Parameters estimation of photovoltaic module using nonlinear least square algorithm: A comparative study," 2013 Annual IEEE India Conference (INDICON), 2013, pp. 1-6, doi: 10.1109/INDCON.2013.6726120.

[13] D. Ben hmamou et al., “Parameters identification and optimization of photovoltaic panels under real conditions using Lambert W-function,” Energy Reports, vol. 7, pp. 9035–9045, Nov. 2021, doi: 10.1016/j.egyr.2021.11.219.

[14] G. N. Psarros, E. I. Batzelis, and S. A. Papathanassiou, “Partial Shading Analysis of Multistring PV Arrays and Derivation of Simplified MPP Expressions,” IEEE Transactions on Sustainable Energy, vol. 6, no. 2, pp. 499–508, Apr. 2015, doi: 10.1109/tste.2015.2389715.

[15] C. Xiao, X. Yu, D. Yang, and D. Que, “Impact of solar irradiance intensity and temperature on the performance of compensated crystalline silicon solar cells,” Solar Energy Materials and Solar Cells, vol. 128, pp. 427–434, Sep. 2014, doi: 10.1016/j.solmat.2014.06.018.

[16] S. Dubey, J. N. Sarvaiya, and B. Seshadri, “Temperature Dependent Photovoltaic (PV) Efficiency and Its Effect on PV Production in the World – A Review,” Energy Procedia, vol. 33, pp. 311–321, 2013, doi: 10.1016/j.egypro.2013.05.072.

[17] M. G. Villalva, J. R. Gazoli, and E. R. Filho, “Comprehensive Approach to Modeling and Simulation of Photovoltaic Arrays,” IEEE Transactions on Power Electronics, vol. 24, no. 5, pp. 1198–1208, May 2009, doi: 10.1109/tpel.2009.2013862.

[18] C. Xiao, X. Yu, D. Yang, and D. Que, “Impact of solar irradiance intensity and temperature on the performance of compensated crystalline silicon solar cells,” Solar Energy Materials and Solar Cells, vol. 128, pp. 427–434, Sep. 2014, doi: 10.1016/j.solmat.2014.06.018.

[19] S. Lun, S. Wang, G. Yang, and T. Guo, “A new explicit double-diode modeling method based on Lambert W-function for photovoltaic arrays,” Solar Energy, vol. 116, pp. 69–82, Jun. 2015, doi: 10.1016/j.solener.2015.03.043.

[20] S. Saravanan and N. Ramesh Babu, “Maximum power point tracking algorithms for photovoltaic system – A review,” Renewable and Sustainable Energy Reviews, vol. 57, pp. 192–204, May 2016, doi: 10.1016/j.rser.2015.12.105.

[21] E. Romero-Cadaval, G. Spagnuolo, L. G. Franquelo, C. A. Ramos-Paja, T. Suntio, and W. M. Xiao, “Grid-Connected Photovoltaic Generation Plants: Components and Operation,” IEEE Industrial Electronics Magazine, vol. 7, no. 3, pp. 6–20, Sep. 2013, doi: 10.1109/MIE.2013.2264540.

[22] M. G. Villalva, J. R. Gazoli, and E. R. Filho, “Comprehensive Approach to Modeling and Simulation of Photovoltaic Arrays,” IEEE Transactions on Power Electronics, vol. 24, no. 5, pp. 1198–1208, May 2009, doi: 10.1109/tpel.2009.2013862.

[23] R. Ayop and C. W. Tan, “Design of boost converter based on maximum power point resistance for photovoltaic applications,” Solar Energy, vol. 160, pp. 322–335, Jan. 2018, doi: 10.1016/j.solener.2017.12.016.

[24] M. Y. Ye and S. Li, “Simulation Study of PFC Boost Converter Based on Predicted Average Current Control,” Advanced Materials Research, vol. 462, pp. 738–742, Feb. 2012, doi: 10.4028/www.scientific.net/amr.462.738.

[25] H. A. Mohamed, H. A. Khattab, A. Mobarka and G. A. Morsy, "Design, control and performance analysis of DC-DC boost converter for stand-alone PV system," 2016 Eighteenth International Middle East Power Systems Conference (MEPCON), 2016, pp. 101-106, doi: 10.1109/MEPCON.2016.7836878.

[26] E. UZLU and T. DEDE, “Jaya algoritması ile optimize edilmiş yapay sinir ağlarını kullanarak Türkiye’de elektrik enerjisi tüketiminin tahmini,” Gazi Üniversitesi Fen Bilimleri Dergisi Part C: Tasarım ve Teknoloji, Jul. 2020, doi: 10.29109/gujsc.684334.

[27] [1]T. H. Kwan and X. Wu, “Maximum power point tracking using a variable antecedent fuzzy logic controller,” Solar Energy, vol. 137, pp. 189–200, Nov. 2016, doi: 10.1016/j.solener.2016.08.008.

[28] “A COMPARISON BETWEEN PERTURB AND OBSERVE AND MODIFIED PERTURB AND OBSERVE MPPT TECHNIQUES,” International Journal of Advance Engineering and Research Development, vol. 4, no. 11, Nov. 2017, doi: 10.21090/ijaerd.30802.

[29] L. Piegari and R. Rizzo, “Adaptive perturb and observe algorithm for photovoltaic maximum power point tracking,” IET Renewable Power Generation, vol. 4, no. 4, p. 317, 2010, doi: 10.1049/iet-rpg.2009.0006.

[30] A. El Khateb, N. A. Rahim and J. Selvaraj, "Optimized PID controller for both single phase inverter and MPPT SEPIC DC/DC converter of PV module," 2011 IEEE International Electric Machines & Drives Conference (IEMDC), 2011, pp. 1036-1041, doi: 10.1109/IEMDC.2011.5994743.

[31] R. Pradhan and B. Subudhi, “Design and real-time implementation of a new auto-tuned adaptive MPPT control for a photovoltaic system,” International Journal of Electrical Power & Energy Systems, vol. 64, pp. 792–803, Jan. 2015, doi: 10.1016/j.ijepes.2014.07.080.

[32] D. Pathak, G. Sagar, and P. Gaur, “An Application of Intelligent Non-linear Discrete-PID Controller for MPPT of PV System,” Procedia Computer Science, vol. 167, pp. 1574–1583, 2020, doi: 10.1016/j.procs.2020.03.368.

[33] Aidan O'dwyer, Handbook of PI and PID controller tuning rules. London: Imperial College Press, Cop, 2009.

[34] J. G. Ziegler and N. B. Nichols, “Optimum Settings for Automatic Controllers,” Journal of Dynamic Systems, Measurement, and Control, vol. 115, no. 2B, pp. 220–222, Jun. 1993, doi: 10.1115/1.2899060.

[35] “Robust advanced PID control (RaPID): PID tuning based on engineering specifications,” IEEE Control Systems, vol. 26, no. 1, pp. 15–19, Feb. 2006, doi: 10.1109/mcs.2006.1580148.

[36] D. S. Karanjkar, S. Chatterji, A. Kumar, and S. L. Shimi, “Fuzzy adaptive proportional-integral-derivative controller with dynamic set-point adjustment for maximum power point tracking in solar photovoltaic system,” Systems Science & Control Engineering, vol. 2, no. 1, pp. 562–582, Oct. 2014, doi: 10.1080/21642583.2014.956267.

[37] Z. Chen and J. Xu, “High boost ratio DC–DC converter with ripple-free input current,” Electronics Letters, vol. 50, no. 5, pp. 353–355, Feb. 2014, doi: 10.1049/el.2013.3984.

[38] AVR System Optimization through Optimum Design of PID Controller,” International Journal of Recent Trends in Engineering and Research, pp. 391–396, Jan. 2018, doi: 10.23883/ijrter.conf.20171225.059.sueuf.

[39] Kiam Heong Ang, G. Chong, and Yun Li, “PID control system analysis, design, and technology,” IEEE Transactions on Control Systems Technology, vol. 13, no. 4, pp. 559–576, Jul. 2005, doi: 10.1109/tcst.2005.847331.

[40] Byung Duk Min et al., "A novel grid-connected PV PCS with new high efficiency converter," 2007 7th Internatonal Conference on Power Electronics, 2007, pp. 478-482, doi: 10.1109/ICPE.2007.4692433.

[41] H. Zhang, L. Shan, J. Ren, B. Cheng and H. Zhang, "Study on photovoltaic grid-connected inverter control system," 2009 International Conference on Power Electronics and Drive Systems (PEDS), 2009, pp. 210-212, doi: 10.1109/PEDS.2009.5385769.

[42] M. A. Memon, “Sizing of dc-link capacitor for a grid connected solar photovoltaic inverter,” Indian Journal of Science and Technology, vol. 13, no. 22, pp. 2272–2281, Jun. 2020, doi: 10.17485/ijst/v13i22.406.

[43] Bhim Singh, (Electrical Engineer, A. Chandra, and Kamal Al-Haddad, Power quality problems and mitigation techniques. Chichester, West Sussex, United Kingdom: Wiley, 2015.

[44] A. Nicastri and A. Nagliero, "Comparison and evaluation of the PLL techniques for the design of the grid-connected inverter systems," 2010 IEEE International Symposium on Industrial Electronics, 2010, pp. 3865-3870, doi: 10.1109/ISIE.2010.5637778.

[45] M. R. Amin, “PLL and Self-Synchronized Synchonverter: An Overview of Grid-Inverter Synchronization Techniques,” International Journal of Simulation: Systems, Science & Technology, Jan. 2016, doi: 10.5013/ijssst.a.17.41.08.

[46] N. E. Zakzouk, A. K. Abdelsalam, A. A. Helal, and B. W. Williams, “PV Single-Phase Grid-Connected Converter: DC-Link Voltage Sensorless Prospective,” IEEE Journal of Emerging and Selected Topics in Power Electronics, vol. 5, no. 1, pp. 526–546, Mar. 2017, doi: 10.1109/jestpe.2016.2637000.

[47] Y. Yang, F. Blaabjerg and Z. Zou, "Benchmarking of Grid Fault Modes in Single-Phase Grid-Connected Photovoltaic Systems," in IEEE Transactions on Industry Applications, vol. 49, no. 5, pp. 2167-2176, Sept.-Oct. 2013, doi: 10.1109/TIA.2013.2260512.